# “I might run into a burning building for the SRS MapCHECK. It keeps us safe in a way we really weren’t safe before.”

*Christopher Bowen, MS, DABR, Mosaic Life Care at St. Joseph, U.S.*

There’s no turning back* once you gain faster, filmless workflows and far greater insights for SRS/SBRT Patient QA.

Join the growing global community of ~400 SRS MapCHECK® users.

**Start here**


** Please don’t run into a burning building, even for an SRS MapCHECK.*

SUN NUCLEAR corporation

Patient Safety Starts Here

# Clinical commissioning of intensity-modulated proton therapy systems: Report of AAPM Task Group 185

Jonathan B. Farr[a)]
*Department of Medical Physics, Applications of Detectors and Accelerators to Medicine, Meyrin 1217, Switzerland*

Michael F. Moyers
*Shanghai Proton and Heavy Ion Center, Shanghai 201315, China*

Chris E. Allgower
*Richard L. Roudebush VA Medical Center, Indianapolis, IN 46202, USA*

Martin Bues
*Department of Radiation Oncology, Mayo Clinic, Scottsdale, AZ 85259, USA*

Wen-Chien Hsi
*University of Florida Proton Therapy Institute, University of Florida, Jacksonville, FL 32206, USA*

Hosang Jin
*Department of Radiation Oncology, University of Oklahoma Health Sciences Center, Oklahoma City, OK 73104, USA*

Dimitris N. Mihailidis
*Department of Radiation Oncology, University of Pennsylvania, Philadelphia, PA 19104, USA*

Hsiao-Ming Lu
*Department of Radiation Oncology, Hefei Ion Medical Center, 1700 Changning Avenue, Gaoxin District, Hefei, Anhui 230088, China*

Wayne D. Newhauser
*Department of Physics & Astronomy, Louisiana State University, Baton Rouge, LA 70803, USA*
*Mary Bird Perkins Cancer Center, Baton Rouge, LA 70809, USA*

Narayan Sahoo
*Department of Radiation Physics, University of Texas MD Anderson Cancer Center, Houston, TX 77030, USA*

Roelf Slopsema
*Department of Radiation Oncology, Emory Proton Therapy Center, Emory University, Atlanta, GA 30322, USA*

Daniel Yeung
*Saudi Proton Therapy Center, King Fahad Medical City, Riyadh, Riyadh Province 11525, Saudi Arabia*

X. Ronald Zhu
*Department of Radiation Physics, University of Texas MD Anderson Cancer Center, Houston, TX 77030, USA*

(Received 10 February 2020; revised 17 August 2020; accepted for publication 18 August 2020; published 17 November 2020)

Proton therapy is an expanding radiotherapy modality in the United States and worldwide. With the number of proton therapy centers treating patients increasing, so does the need for consistent, high-quality clinical commissioning practices. Clinical commissioning encompasses the entire proton therapy system's multiple components, including the treatment delivery system, the patient positioning system, and the image-guided radiotherapy components. Also included in the commissioning process are the x-ray computed tomography scanner calibration for proton stopping power, the radiotherapy treatment planning system, and corresponding portions of the treatment management system. This commissioning report focuses exclusively on intensity-modulated scanning systems, presenting details of how to perform the commissioning of the proton therapy and ancillary systems, including the required proton beam measurements, treatment planning system dose modeling, and the equipment needed. © *2020 American Association of Physicists in Medicine* [https://doi.org/10.1002/mp.14546]

Key words: calibration, commissioning, IMPT, modulated scanning, PBS, proton, scanning

TABLE OF CONTENTS

1. TERMINOLOGY
2. INTRODUCTION
3. PURPOSE AND SCOPE OF THIS REPORT
4. EDUCATION, TRAINING, AND TIMING
4.A. Didactic education
4.B. Practical training
4.C. Timing
5. COMMISSIONING A CT SCANNER FOR PROTON THERAPY PLANNING
5.A. Background
5.B. CTN to RLSP conversion for proton beams
6. ANCILLARY DEVICES AND MATERIALS
6.A. Treatment tabletops
6.B. Immobilization devices in proton therapy
*6.B.1. Mitigating range uncertainty due to immobilization devices*
*6.B.1. Specialized immobilization devices*
6.C. High–atomic number materials in proton beams
7. COMMISSIONING IMAGE GUIDANCE SYSTEMS FOR PROTON THERAPY
7.A. Planar image guidance
7.B. Volumetric image guidance
8. TREATMENT MANAGEMENT SYSTEM COMMISSIONING
8.A. Background
8.B. Commissioning
9. PROTON MACHINE ABSOLUTE DOSE CALIBRATION
9.A. Radiobiological effectiveness factor
9.B. Calibration protocol
9.C. Reference field and point of measurement
9.D. Ionization chamber choice and associated uncertainties
*9.D.1. 60-Co ionization chamber calibration uncertainty*
*9.D.2. Long-term ionization chamber stability uncertainty*
*9.D.3. Calibration ionization chamber choice and absolute dosimetry uncertainties*
9.E. Interfacility comparisons and remote auditing
10. OUT-OF-FIELD DOSE FROM PROTON THERAPY
11. RADIOTHERAPY PLANNING SYSTEM COMMISSIONING
11.A. Dose modeling for treatment planning
*11.A.1. Analytical dose model representation*
*11.A.2. Modeling low-dose halo*
*11.A.3. Accuracy and limitations of analytical dose algorithms*
*11.A.4. Monte Carlo as a dose model for treatment planning*
11.B. Apertures and energy absorbers
11.C. Dose normalization to absolute dose
11.D. Dose model data acquisition
*11.D.1. Integral depth-dose measurement, scaling, and corrections*
*11.D.2. Spot profiles*
*11.D.3. Virtual source–to-axis distance*
*11.D.4. Energy absorbers*
*11.D.5. Ripple filters*
*11.D.6. Apertures*
11.E. Monitor unit determination
11.F. Beam model verification
11.G. Role of Monte Carlo in data modeling
12. END-TO-END VERIFICATION
12.A. Scope of end-to-end verification
12.B. End-to-end testing methods and materials
12.C. End-to-end testing details
13. POSSIBLE COMMISSIONING ERRORS AND MITIGATIONS
14. SUMMARY OF RECOMMENDATIONS

## 1. TERMINOLOGY

The development of proton therapy has resulted in extensive specialized terminology. This report follows the terminology set forth in the American Association of Physicists in Medicine (AAPM) Summer School monograph *Principles and Practice of Proton Therapy.*[1] Table I lists the related terminology used in this report.

## 2. INTRODUCTION

Proton therapy is a radiotherapy modality that is being used increasingly in the United States and worldwide. As the number of proton therapy centers treating patients increases, so does the need for consistent, high-quality clinical commissioning standards and procedures.

Clinical commissioning addresses multiple components of the proton therapy system (PTS), including the treatment delivery system (TDS), the patient positioning system (PPS), and the image-guided radiotherapy (IGRT) components. Also, the commissioning process includes calibration of the x-ray computed tomography (CT) for stopping power determination. Beam modeling and verification are needed for the treatment planning system (TPS), as well as configuration and verification of the corresponding portions of the treatment management system (TMS), which is also sometimes termed the oncologic information system (OIS).

If beam-modifying devices are used, their manufacture and dosimetric characterization are also included in the commissioning process. Today's PTSs are highly integrated; therefore, commissioning activities should ensure the proper operation of the various individual subsystems, as well as of the complete integrated system. Lastly, commissioning also includes the development of system-specific and patient-specific quality assurance (QA) procedures and user training. System-specific QA, as well as a general description of proton therapy systems, is addressed elsewhere.[2]

## 3. PURPOSE AND SCOPE OF THIS REPORT

New proton therapy centers use intensity modulated proton therapy (IMPT). This report provides specific details on how to perform the commissioning of IMPT systems. The required proton beam measurements and the techniques and equipment necessary to collect them are provided.

The use of scanning systems for ocular applications is a developing application,[3] as are scanned proton mini-beams,[4] and both are outside the scope of this report. Also, the

TABLE I. Proton therapy–specific terminology.

| Term (recommended) | Abbreviation/ acronym | Definition | Alternate term |
|---|---|---|---|
| Aperture | | The non-attenuating opening in a collimator, shaped irregularly according to the shape of the target, that allows radiation to reach a target | Collimator |
| Beam | | A group of particles or rays traveling in the same direction in parallel or diverging from a point | |
| Beam energy | | The energy at the treatment head (nozzle) entrance. This is a generic term that may also specify the beam at positions other than the treatment head, in which case this should be stated | |
| Beam energy spread | | The energy spread (sigma) at the treatment head entrance. This is a generic term that may also specify the beam energy spread at positions other than the treatment head, in which case this should be stated | |
| Beamline | | A device or combination of devices used to deliver a beam from an accelerator to a specific location (e.g., a treatment room) | |
| Beamlet | | (For scanning beams and IMPT). A monoenergetic particle beam of small cross-section that enters the nozzle and reaches the patient or phantom without being scattered or modulated. A range shifter may be inserted to reduce the range. Another term, "pencil beam," has become common in the field of particle therapy. For instance, "pencil-beam scanning," or PBS, is used to describe scanning beams. Therefore, either "beamlet" or "pencil beam" may be used. However, because the term "pencil beam" is also used to refer to a conceptual tool in dose-calculation algorithms, its use to describe the beam of particles entering the scanned delivery should be clearly indicated | Pencil beam |
| Bragg curve | | The depth-dose curve for a beamlet beam, or the depth-dose curve of a broad beam of quasi-monoenergetic charged particles | |
| Bragg peak | | The narrow, high-dose region at depths near the maximum dose on a Bragg curve near the end of proton range | |
| Control point | CP | CP is a DICOM RT term. It refers to a delivery device that changes setting during delivery. For instance, in pencil-beam scanning, CP specifies the positions and weights for a collection of spots in a given energy layer | |
| Distal fall-off region | | The distal part (beyond the Bragg peak or SOBP) of the particle depth-dose curve | |
| Distal penumbra | | The distance between the depth of a specific percentage of the dose at the Bragg peak (or SOBP) and the depth of a lower percentage of the Bragg peak (or SOBP) dose in the distal fall-off region. Typically, the distal penumbra is defined as the distance between the 80% and 20% dose values | |
| Energy absorber | | A block of low atomic number material of uniform thickness inserted in a beam for the purpose of reducing the energy (and range) of the beam. In some cases, an energy absorber is placed near the patient to preserve penumbral sharpness | Pre-absorber, range shifter |
| Gy (RBE) | Gy (RBE) | The product of the physical dose in Gy and the RBE used as the unit of dose | Cobalt Gray equivalent (CGE); is an alternative, similar quantity that is superseded by Gy (RBE) |
| Halo | | The low-level secondary particle radiation field extending outside the lateral and distal penumbrae of a primary beam. The halo may contain components from the machine and the patient | Nuclear halo |
| Integral depth dose | IDD | The integral of the dose on an infinite plane normal to the central axis of a beam, beamlet or an infinitesimal pencil beam. It is represented as a function of depth | |
| Intensity-modulated proton therapy | IMPT | One of the multiple modes of proton therapy planning and delivery methods in which scanned beamlets of a sequence of energies and of optimized intensities are used to achieve an appropriate balance between the target dose and the normal tissue doses | |
| Lateral penumbra | LPxx-yy (e.g., LP80-20) | The distance between the point at which the dose is a certain percentage of the central axis value and the point at which the dose is a lower percentage of the central axis value. Typically, the penumbra is defined as the distance between the 80% and 20% dose values | |
| Layer | | The irradiation with a scanned monoenergetic beam of protons | |
| Linear stopping power | LSP | The energy lost by a charged particle in traversing a unit distance in the medium | $dE/dx$ |

TABLE I. Continued.

| Term (recommended) | Abbreviation/ acronym | Definition | Alternate term |
|---|---|---|---|
| Matched treatment rooms | Twinned treatment rooms | Treatment rooms that are dosimetrically and physically equivalent within acceptable tolerances | |
| Modulation width | | The distal dose fall-off position minus the proximal dose fall-off position in a SOBP in water. The position has to be explicitly stated, for example, "98−90," reflecting a 98% proximal dose fall-off position minus a 90% distal dose fall-off position | SOBP width |
| Multiple Coulomb scattering | MCS | The primary scattering process of protons, which is due to electrostatic interactions with nuclei. Multiple small-angle deflections of charged particles traversing a medium due to Coulomb scattering from nuclei result in the lateral spreading of proton beams | |
| Multi-layer ionization chamber | MLIC | A device similar to a Multi-Layer Faraday Cup (MLFC) but consisting of multiple layers of parallel plate ionization chambers, providing a fixed WET separation. As with an MLFC, an MLIC allows rapid range measurement before beam delivery to the patient. It is also used for off-line quality assurance purposes | |
| Nozzle | | The part of a beam delivery system in the treatment room (attached to the gantry in rooms with gantries) into which the narrow beam of protons enters, which houses the beam-shaping and dose-monitoring equipment and from which the radiation emerges | Treatment head |
| Patient positioning system | PPS | The physical device that supports the patient and moves them into the treatment position. It usually has 6 degrees of freedom of motion | |
| Pencil beam | | A mathematical construct comprising a monoenergetic beam of particles with an infinitesimal lateral dimension and angular emittance at the point of consideration (e.g., at the point of incidence on the patient). The pencil beam construct used in an algorithm to calculate dose distributions for large fields. (Note the distinction between a pencil beam and a beamlet. Many authors use the term "pencil beam" to mean a beamlet, that is, a beam of small cross-section. The pencil beam may be called the "infinitesimal" or "calculational" pencil beam. To avoid confusion, the intended meaning of "pencil beam" should be clearly stated.) | |
| Plateau | | The relatively uniform region of a depth-dose distribution between the surface and the SOBP of a range-modulated beam or between the surface and the peak of a non–range-modulated (pristine monoenergetic) beam | |
| Pristine beam | | A monoenergetic, unscattered beam of particles. It may be a single beamlet or a beam composed of uniformly scanned beamlets of the same energy. The term may also be used for beams that have a narrow and symmetric energy spread | |
| Nonlinear Response Saturation | | In ionizing radiation detection, the phenomenon that can occur when the detector/sensor no longer responds in proportion to absorbed dose, for example, recombination in an ionization chamber and quenching in a scintillator | |
| Range | Rxx (e.g., R80 or R90) | The mean penetration depth of a charged particle beam. In this report, we define range as the depth at which the absorbed dose of a beam falls off to a fraction of the maximum value just beyond the Bragg Peak. Range increases with beam energy and decreases with the mass density and linear stopping power of the absorber. Consequently, it is convenient to specify range values in liquid water at unit density. For comparison with traditional range tables from the literature, R80 is used. For clinical purposes, R90 is commonly used. In the literature, range has been defined in many ways, for example, the depth at which half of all incident particles have come to rest. Because of the myriad usages of the term "range" in the literature, great care must be used to ensure proper interpretation of the intended meaning | |
| Range shifter | | See energy absorber | |
| Range uncertainty margin | | Distal and proximal margins with respect to the treatment target, to account for uncertainties in the calculated and/or delivered range of particles for fulfilling prescribed target doses | |

TABLE I. Continued.

| Term (recommended) | Abbreviation/ acronym | Definition | Alternate term |
|---|---|---|---|
| Relative biological effectiveness | RBE | The ratio of absorbed doses necessary to obtain the same biological effect from photon beams and proton beams. RBE values vary with organ or tissue, dose, and a variety of host and treatment factors. Scientific evidence on RBE values in humans is sparse and highly uncertain. In lieu of observed RBE data in humans, values have been "recommended" based on available knowledge and subjective judgement | |
| Relative linear stopping power | RLSP | The linear stopping power value of a proton beam in some material relative to the corresponding value in liquid water | |
| Repainting | | A scanning beam technique whereby the beam scans the same volume multiple times during a treatment with the intent being to average mitigate against the deleterious effects of any patient motionthat was not fully taken into account in treatment planning and deliver. The term may also be used for the practice of scanning each energy layer multiple times before proceeding to the next layer | Re-scanning |
| Residual range | | The remaining range of particles at a point of interest, either in the phantom or in the patient. It is the difference in depths between the range and a point of interest. Like range, for convenience, it is commonly expressed in residual range in water | |
| Ridge filter | | A range modulator that consists of several ridges and valleys that present different thicknesses of material to an incoming beam in order to vary its penetration into the patient | |
| Ripple filter | | A range modulator (typically a thin ridge filter) that produces just enough variation in the light ion energies entering the patient that a reduced number of accelerator energies may be used without producing ripples in the depth-dose distribution | |
| Robust optimization | | A method to take into account uncertainties in order to optimize a planned dose distribution to be resilient to uncertainties in planning and delivery | |
| Robustness | | A measure of the resilience of a dose distribution to uncertainties | |
| Scan pattern | | A pattern of scanning, including spot positions, energies, and intensities | |
| Scanned beam | | A narrow beam that is laterally scanned to increase the irradiated volume | |
| Snout | | The most distal part of the treatment head (nozzle) to which interchangeable beam applicators (e.g., apertures and compensators) are attached and which may extend toward and retract away from the isocenter. The snout moves parallel to the central axis of the beam | Aperture carriage |
| Spot | | A proton beamlet at a specified beam energy and lateral position | |
| Spot profile | | The two-dimensional representation of a spot in air or at depth in a medium. Its significant features are its size, its circularity, and its 1st and 2nd Gaussian fit parameters | |
| Spot scanning | | A technique for creating a large field by scanning a beamlet spot across the target volume. The beamlet stops at each predetermined point and delivers a specified dose. Irradiation is usually switched off between the points of delivery | Discrete scanning |
| Spot spacing | | In scanning beam treatments, lateral spacing between centers of uniformly spaced spots placed in the target volume | |
| Spread-out Bragg peak | SOBP | The depth-dose distribution resulting from a combination of a set of quasi-monoenergetic beams. The intensities are chosen to produce a region of longitudinally and laterally flat dose distribution in order to cover a target of a finite size in depth | |
| Stopping power ratio | SPR | The stopping power of a medium for a particle of given energy and type is defined as the average energy loss of the particle per unit pathlength and is typically expressed in units of MeV/cm. The stopping power ratio is the ratio of the stopping power of a medium to that of water | |
| Treatment delivery system | TDS | This term pertains to all components related to the physical and control-system aspects of delivering proton beam irradiation | |
| Treatment management system | TMS | Also known as an oncologic information system. The system responsible for transferring patient-specific DICOM-RT-ION data from the radiotherapy planning system to the treatment delivery system. The TMS also serves to handshake interlock values with the treatment delivery system, record treatment data, and provide partial delivery recovery | OIS |
| Water equivalent thickness | WET | The range of a proton beam in water that corresponds to the thickness of a specific material that leads to the same mean energy loss | |

radiobiological aspects of proton therapy are covered by the dedicated *TG-256*.[5]

In general, final acceptance testing should precede clinical commissioning. This may not always be possible, for example, when multiple delivery or imaging methods are commissioned in sequential order, and some of the commissioning is not completed until a later date. It is also prevalent for multiroom centers to commission and open treatment rooms in sequential order to better meet the clinic's immediate needs. This report's scope does not include acceptance testing[6–8] or safety programs (mechanical and radiation), both of which are required before commissioning. Usually, portions of the safety testing are required as part of the application process for the facility operating permission. Detailed information on acceptance testing, including safety testing, is available elsewhere.[9] Also, guidance about the activation hazards associated with proton therapy is available elsewhere.[10] Lastly, the American College of Radiology (ACR) recently published a document on technical standards on proton therapy.[11]

Although this report focuses on the clinical commissioning of IMPT, it is not intended to describe IMPT systems in detail as such information is available elsewhere.[2,12] Instead, the intent is to systematically review the technical commissioning needs of a new proton therapy system, including ancillary devices such as image guidance (IG) equipment and the TMS. Very basic systems, such as room lasers are not covered, and advanced functionality, such as treatment planning techniques, motion management, gating, and target tracking, are left to future reports. Broader descriptions of measurement devices for use in proton therapy are available elsewhere.[13,14]

One of the main tasks of commissioning is preparing the TPS for clinical use. Some fundamental physical (non-dosimetric) parameters are required. These values are available from the equipment vendor.[15,16] Commissioning a TPS usually requires two categories of measured data: those specified by the planning system as being inputs needed for building the beam models and those used to verify the calculated dose distributions and refine the beam model, if necessary. When selecting verification measurements for the beam model and calculated dose distributions, one should consider the related limitations, the relevance of the measurement to clinical applications, the number of measurements, and how the inclusion of a proposed measurement will affect the time frame for completing the commissioning task. In general, the processes of dosimetric measurements and analysis are time-consuming, especially when discrepancies arise. Monte Carlo (MC) modeling is used more frequently than in the past to understand unexpected measurement results and provide a valuable second reference. Although MC modeling is not required for commissioning, details of its use are included in this report because of its potential to reduce error and increase efficiency. Also, commercial MC dose calculation for proton beams is beginning to enter clinical practice. Finally, the report includes details on end-to-end testing and commissioning recommendations.

## 4. EDUCATION, TRAINING, AND TIMING

It is recommended that the commissioning team members (the team) receive training in proton therapy. The training has several components.

### 4.A. Didactic education

Didactic educational material on general proton therapy principles and practice can be found in various resources.[17–20] The team should also ideally attend an educational course such as the education sessions offered by the Particle Therapy Co-Operative Group (PTCOG) or the AAPM annual meetings.

### 4.B. Practical training

Before commencing acceptance testing and commissioning, a vendor's partner sites can offer observational training with the advantage of direct experience with the same type of equipment to be used by the team.

Direct participation in acceptance testing before commissioning is probably of the highest practical operational value. The user is encouraged to become actively involved during the acceptance-testing phase taking advantage of the direct vendor assistance available during the period to assist them with operating the equipment, whereas, during clinical commissioning, vendor assistance may be limited to an indirect supporting role. The vendor should train the team in the specific operation of their proton therapy equipment. Also, the team should be trained by the vendor on the dosimetry equipment and systems.

Before commissioning a proton therapy system, it is recommended that the user become fully aware of the features, properties, and limitations of all sensors and detector (ionization chambers, scintillation systems, films, etc.) used in proton beam measurements. For ionization chamber–based detectors, the factors to consider are appropriate bias, correction for recombination, and selecting an appropriate size and shape of chamber.[21] Integrating sensors such as film or scintillating systems require care to avoid saturation in high linear energy–transfer regions,[22–24] spatial deviations over the scan or capture area, and artifacts near the edges.[25,26]

It is recommended that the new proton beam user setup the TPS as early as possible for planning practice. Proton TPSs typically come with installed sample data, which is sufficient to begin rough exercises. MC–generated data (Section 11.G) can provide near realistic beam data[27] that can be verified and/or improved later with commissioning measurements. Given the difficulty of discerning the quality of novice proton treatment planning efforts, external review by experienced planners is recommended, before a system is first used to treat a patient. Also, the reviewers, which should be a multidisciplinary team (including radiation oncologists and medical physicists), should review and suggest improvements for the proposed proton treatment planning policies and

TABLE II. Example of a commissioning schedule for a one-room IMPT installation. Most of the activities require proton beam irradiations. Some activities not requiring proton irradiations (†) may be performed earlier in the facility if access is available.

| | Objective A | Objective B | Objective C | Milestone |
|---|---|---|---|---|
| Week 1 | Machine dose calibration | Test all commissioning equipment and setups used† | | Dose calibration |
| Week 2 | Beam measurements | Daily output check | Calibrate CT simulator† | 2-week clinical machine stability achieved |
| Week 3 | Beam measurements | Image guidance debugging and optimization† | | |
| Week 4 | Beam measurements | Image guidance debugging and optimization† | | |
| Week 5 | Beam measurements | | Dose modeling | Beam model measurements completed |
| Week 6 | Image guidance debugging and optimization† | Machine-specific quality assurance development | Dose modeling | Image guidance operating correctly |
| Week 7 | Dose model validation | Image guidance exercises† | Machine-specific quality assurance development | |
| Week 8 | Dose model validation | Image guidance exercises† | Machine-specific quality assurance development | Dose model validated |
| Week 9 | End-to-end testing | IROC TLD irradiations | Patient-specific quality assurance development | |
| Week 10 | End-to-end testing | Patient-specific quality assurance development | Staff training† | End-to-end tests complete |
| Week 11 | Mock treatments of initial patient types | Staff training | Quality assurance | Clinical commissioning complete |

procedures and a representative sample of plans covering the intended sites for treatment.

### 4.C. Timing

The commissioning time required for proton therapy systems is a function of the machine complexity, readiness, and staff experience. The example presented in Table II shows how quickly a single IMPT treatment room can be commissioned. The example is calculated based on the experience of commissioning using 12-hr shifts (with two staff members per shift) in the treatment room for 6 days each week. It excludes the commissioning of a nozzle-mounted energy absorber (EA).

The example can be extended to multiple rooms, where further efficiency can be achieved if the systems' calibration fields are within 1% of each other, the spot profiles match within 10%, and the range and absolute mechanical alignments are within 1 mm. The methods to achieve "room matching" relates to the design, installation, and need to be agreed contractually with the PTS provider and installer. Matched or "twinned" treatment rooms provide the additional advantage of seamless patient transfer between treatment rooms in the event of room maintenance or schedule demands. Also, it should be noted that when used for clinical operation, due to reduced room availability times after the commissioning of the first treatment room is completed in a multi-room system, that the commissioning of subsequent rooms may take longer calendar time.

## 5. COMMISSIONING A CT SCANNER FOR PROTON THERAPY PLANNING

### 5.A. Background

In proton therapy, a CT is used to obtain the TPS's volumetric patient data; therefore, it is recommended that the CT scanner used is commissioned as a radiotherapy simulation scanner (CT simulator). Commissioning a CT scanner for TPS simulation requires proton therapy-specific items, as presented in the following subsections. Evaluation of the imaging dose is also part of the process.[28–33] TG-202 discusses the uncertainties associated with the use of a CT scanner in the proton therapy treatment planning process.[34]

### 5.B. CTN to RLSP conversion for proton beams

The CT number (CTN) to relative linear stopping power (RLSP) conversion functions should be determined to provide accurate proton plan optimization and dose calculations. The three most common types of functions that have been used to relate these parameters are the following: (a) direct user input of CTN/RLSP number pairs[35]; (b) direct user input of CTN-to–mass density values, followed by the use of a preprogrammed mass density–to-RLSP function[36]; and (c) direct user input of CTN/tissue group/mass density triplets that are then used to calculate the RLSP.[37–40] The input requirements of the TPS determine the type of function used. The CTN and RLSP measurements of real tissues are difficult to obtain. Therefore, most clinical facilities have used plastic

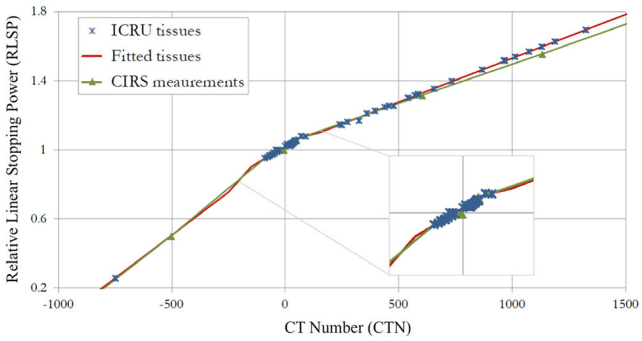


FIG. 1. Plot of relative linear stopping power (RLSP) vs. CT number (CTN), illustrative of the uncertainty arising from manmade polymer inserts relative to calculations from ICRU-46 tissues. [Color figure can be viewed at wileyonlinelibrary.com]

tissue substitute measurements to determine the required proton beam energy for the desired range in a medium. A standard phantom should be used, and verification of the CTN-RLSP fit from the Imaging and Radiation Oncology Core (IROC) Houston Quality Assurance Center* is recommended. As shown in Fig. 1, a plot of the measured CTN/RLSP number pairs for these plastic substitutes does not lie on the function curve for calculations from real tissues, so offsets should be used to convert the measured data to that of real tissue.[35]

The most common conversion function used in TPSs is type (a) given above. The information for this function may be acquired by several different methods, as described by several investigators for both kilovoltage and megavoltage CT.[41–46] Conversion type (b) is more straightforward as it only relates CTN to physical density, but the user may have to manipulate data to have control over the final conversion. Conversion type (c) is usually used with MC dose algorithms.

The accuracy of the conversion is a current concern in the field. In an IROC study, a simplified method and phantom were used to survey 14 scanner conversion functions at ten proton facilities in the United States.[47] Compared to the functions generated using the standard phantom and method, the RLSPs converted using the facility functions varied by 8% for tissues within 300 CTN of water and by 16% for lung tissue. For the conversion of low-density immobilization foam, the facility-to-facility differences were as high as 40%.[48] Although individual institutions claim a 1–2% accuracy for their conversion functions, this study with a standard phantom underscored the difficulty of determining these functions and their variability. These difficulties further support the recommendation to use a similar standard phantom for easy determination of the conversion functions. The IROC is also pursuing the use of a particular phantom with the eventual goal of standardization.[49]

Further advances may be made using dual-, multi-, or spectral-energy CT calibrations that give an effective atomic number and relative electron density.[50–55] However, these methods are still mostly in the research stage and not yet implemented in the clinic. In current practice, using single-kV calibration, the resulting conversion functions should be accurate to within ±2% for soft tissues with near unit density. Other biological tissues with higher or lower density (such as lung) and high Z (such as teeth), will not fall within this range.[46,56] Note that the uncertainty in converting CTN to RLSP is only one component of the overall beam penetration uncertainty. The uncertainty in the CTN itself is typically larger than the conversion uncertainty. Beam delivery inaccuracies also contribute to penetration uncertainty. Also, a separate conversion function should be generated for each set of CT scanner parameters (protocols) with different kVp, scan field-of-view size, and reconstruction kernel.

## 6. ANCILLARY DEVICES AND MATERIALS

Proton therapy treatments are highly conformal. Any unplanned change in pathlength due to the presence of foreign materials can cause severe dose and range errors.[57,58] Whenever a foreign material is introduced into the proton beam, it is recommended to account for the resulting change in beam-path length. Some examples of foreign materials and strategies for accounting for their range-loss properties are presented here, with most materials intended for radiation oncology treatment fabricated from low-density materials. Even so, lightweight devices may have a water-equivalent thickness (WET) of several millimeters, which is sufficient to affect the intended dose distribution if unaccounted for[59]. In addition to the discussion here, the reader is referred to the relevant literature,[60–62] specifically *TG-176*,[63] and the *AAPM Summer School Monograph #37*, Chapter 18, *Immobilization and Simulation*.[59]

### 6.A. Treatment tabletops

It is recommended that the alignment, uniformity, and WET be determined for each tabletop used for therapy. Also, their mechanical sag characteristics with distributed weights should be characterized. Because material inserted between the proton therapy system and the patient reduces proton penetration and scatters the beam, it is recommended that the effect of the treatment couch be considered in cases in which the beam passes through it. A further complication arises if the treatment couch differs from the couch used for TPS simulation.[64] Therefore, a set of physical and radiologic tests should be carried out to ensure the uniformity of the treatment couches to be used. The first step is to acquire a CT scan of each couch and inspect the image set for inhomogeneities resulting from the fabrication process (there should not be any). The second step is to obtain a series of WET measurements at regular spacing through the couch and at several energies.[35] Typically, WET values for commercial treatment couches used in proton therapy range from 0.55 to 1.2 cm. WET, however, is not energy independent.[65,66] The WET angular dependency follows the inverse cosine function from the beam incidence relative to the couch's normal

*IROC Houston QA Center, M. D. Anderson Cancer Center, Unit 607, 1515 Holcombe Blvd, Houston, TX 77030

vector. Because the function is nonlinear and begins to vary greatly at high angles, such high angles of incidence should be avoided. Also to be avoided are the couch edges. Some TPSs can model the treatment couch in place of the scanner couch, as part of the patient-plan preparation process. In such cases, the WET-loss TPS modeling should be verified for the therapy couch.[64]

## 6.B. Immobilization devices in proton therapy

It is well understood by the practitioners of proton beam therapy that proton beams are more sensitive to patient setup uncertainties than conventional external beams.[67] The sensitivity of proton beam therapy plans to setup uncertainty is related to the dependence of the Bragg peak dose deposition curve on depth in the patient. Due to the treatment quality sensitivity to range accuracy, it is essential to appropriately select and characterize the immobilization devices used in proton beam therapy.

### *6.B.1. Mitigating range uncertainty due to immobilization devices*

Any immobilization device in the beam's path should be investigated for its proton stopping power, if possible, through direct measurement in the beam.[68] If the measured stopping power differs significantly from the stopping power predicted by the Hounsfield Unit (HU) to stopping power conversion tables used in the clinic, the immobilization device must be contoured and assigned a HU consistent with the measured stopping power. It is well known that HU estimation may become unreliable at distances far from the CT scanner axis. Therefore, bulky immobilization devices such as oversized vacuum bags that extend into regions of high HU uncertainty should be avoided.

Another way in which immobilization devices may contribute to range uncertainty is by introducing sharp gradients in stopping power in directions perpendicular to the beam direction. If the patient is positioned differently relative to the relative position during CT, such an immobilization device could act as an unintended range shifter, thereby significantly distorting the desired dose distribution. Therefore, immobilization devices used in the proton practice should ideally be chosen with rounded edges.

### *6.B.2. Specialized immobilization devices*

Every immobilization device used for external beam radiation therapy should be evaluated for their ability to reduce the intra- and inter- fractional setup uncertainties. In general, immobilization devices, both internal and external, should cause no or minimal imaging artifacts. Additionally, as described earlier, the effect of the change in the shape, size, and material in the immobilization devices in the proton beam's path can perturb the delivered dose from the planned dose. Therefore, site-specific immobilization devices need to be evaluated for their suitability to be used with proton therapy during their clinical commissioning. Some of the commonly used immobilization devices for treating different sites are described below, with specific recommendations for their evaluation.

*Treatment sites in the pelvis and extremities:* It is preferable to keep immobilization devices out of the beam path. In practice, it is often not possible to do so. For treatment sites in the pelvis, like the prostate, the devices do not come into the beam path. However, the vacuum cushion system can potentially be in the beam path for some non-prostatic sites in the pelvis and for treating targets in the leg, hand, and pelvic area for pediatric patients. Therefore, the vacuum cushion stability during treatment needs to be evaluated, and the ability of the TPS to correctly determine the WET of the material from CT scans should be evaluated.

Internal immobilization, such as the endorectal balloon (ERB), is commonly used during prostate proton beam therapy, often in conjunction with fiducial markers, to control the position of the prostate and rectal mucosa.[69] Recently, gels have become available to separate the prostate from the rectum.[70] These devices must be investigated for their effect on the dose distribution if the proton beam passes through them. Specifically, the procedure for insertion of ERB should be evaluated in the initial stage of its implementation with repeated imaging studies to ensure that the variations in the position of ERB and volume of liquid material in the ERB are minimal. The material of fiducial markers should produce no or minimal imaging artifacts. The spacer gel's WET should be measured and should agree with the calculated value from the TPS from CT images with the gel.

*Treatment sites in the thorax and abdomen:* Thoracic and abdominal patients use similar immobilization devices that may include a sizeable hemi-body vacuum cushion, a wing board, and a T-bar. The wing board and T-bar are always kept out of the beam path. The evaluation of the vacuum cushion's suitability for proton therapy is already described in the previous section. Implanted fiducial markers are also used to localize the targets in the liver and lung. These markers should be evaluated to ensure that they cause no or minimal artifacts, and the TPS correctly calculates the WET of the markers.

A device used as the surrogate of the breathing-related motion may be required to be placed on the patient. However, its location is usually away from the beam path. If it happens to be in the beam path, its WET should be determined by measurement and be compared with the calculated value from TPS using a CT scan taken with the device.

The quantification of any residual uncertainties is important for mitigating these uncertainties in the TPS by using appropriate margins around the target to create planning target volumes or beam specific planning target volumes and plan robustness analysis. This can be achieved by repeated imaging studies and a retrospective study of setup images used for localization before treatment.

*Treatment sites in head and neck, and brain:* Head and neck and brain immobilization devices usually include a headrest, mask, and sometimes a bite block that might require dental stents. All these devices are typically made of low-Z materials and do not create any imaging artifacts. The WET of these devices should be measured and compared with the values calculated by the TPS from the CT images taken with these devices to validate the calculation's accuracy.

### 6.C. High–atomic number materials in proton beams

Metallic objects such as dental fillings or implants can cause CT artifacts. For example, streak artifacts from hip prostheses can lead to range errors of 5–12 mm.[71] Solutions proposed to correct these artifacts and minimize the resulting uncertainties include contour and override suppression algorithms,[72] and the incorporation of megavoltage CT for imaging.[71] Dual-energy and megavoltage CT can also be helpful in this regard.[73–77] The contour and override solutions are the most commonly used methods. A structure of the high-density object is created with the TPS with an assigned HU. If a physical sample of the material can be obtained, a relative range-loss measurement can be performed by placing the sample material in and out of the proton field and noting the difference in range measurements. This is a direct RLSP determination. It is recommended to override the density of high-atomic number materials by using a measured RLSP corresponding to the CTN from the CT-simulator calibration. In some cases, the RLSP-to-CTN curve should be extended to higher values to include special materials. It can also be important to contour and override normal low atomic number tissues with significant imaging artifacts from adjacent high atomic number materials and reassign HU values for them compared to the same tissues outside regions of heavy metal artifacts.

Although the TPS may calculate a correct beam range through metal objects, it may still underestimate the lateral scattering of protons caused by these objects. Unless MC modeling is used, the user should be cautious when evaluating doses to organs at risk (OARs) located lateral and distal to the metal objects. When treating through high-density materials, single-field treatment plans should be avoided. Because MC dose modeling has recently become available in commercial TPSs, its use is suggested in these cases.

Based on the results of modeling, suitable margins and an appropriate number of fields should be used to provide sufficient robustness against range uncertainty and dose shadow effects.

## 7. COMMISSIONING IMAGE GUIDANCE SYSTEMS FOR PROTON THERAPY

Planar kV IG is currently the most commonly used type in proton therapy. Volumetric kV IG is also used, and its use is becoming more widespread.[78] Other developmental IG or "direct" image verification systems include surface (or its surrogate) imaging systems, proton imaging,[79–91] prompt gamma (p,γ) imaging,[92–100] and proton-PET (p,β+).[101–109] If any of these complementary systems are to be used clinically, then special care must be taken during commissioning to align the complementary system to the standard system. The present report restricts itself to the commissioning of standard kV IG systems.

Most of the kV IG systems used in proton therapy communicate directly with the PPS to position the patient daily or field-by-field. It is recommended that the accuracy of the PPS and IG system, including the accuracy of isocentric motion, be verified by acceptance testing before clinical commissioning. Proton therapy IG commissioning aims to achieve the following: correct spatial orientation of the TPS, IG, and delivery system for all geometries treated; adequate image quality with optimized clinical parameters; minimized doses for the use cases; and sufficient staff experience with the IG process. Additional verification of the IG system is performed as part of the end-to-end testing. Useful tools for commissioning planar and volumetric IG systems are presented in Table III.

Although IG applications parallel conventional therapy, they are usually different in appearance and sometimes in operation. Enough time and support should be given to the therapy staff to become familiar with the IG process. Part of the process determines the clinical guideline for when the IG alignment accuracy is sufficient for treatment. A setup accuracy guideline range is recommended that is synchronized with the treatment plan margins and robustness.

### 7.A. Planar image guidance

The distances from the source to the isocenter and detector should be known in terms of their magnification effect. Images acquired by x-ray systems are typically compared to reference digitally reconstructed radiographs (DRRs) from treatment planning.[110–112] In some cases, DRRs may be

TABLE III. Image guidance commissioning tools.

| Device | Imaging type | Comments |
|---|---|---|
| X-ray test object | 2D | Radiographic image quality |
| 2D-alignment test object | 2D | Planar geometric alignment |
| X-ray source quality object | 1D | kVp accuracy, linearity, and reproducibility |
| 3D volumetric test object | 3D | Volumetric image quality |
| 3D-alignment test object | 3D | Volumetric geometric alignment |
| CT ion chamber | 3D | CT integral dose (CTDI) |
| Anthropomorphic phantom | 2D + 3D | Suitable for proton therapy use |
| Laser tracker | 2D + 3D | Optional but helpful |

generated at the imaging console directly from planning DICOM-RT data. The images are then compared by aligning the acquired images with the planned DRR images, most commonly concerning the bony anatomy or implanted fiducial markers. The amount of translational and/or angular shifting needed to match the images is used to calculate the correction vector applied to the PPS. After the corrective movement, the patient position may be verified (or not) by re-imaging, depending on the clinic policy. The use of internal fiducial markers instead of or along with bony anatomy should be considered part of clinical preparation.[113] Markers come in many varieties: some are bio-oncotic, and some are simple metallic structures. As there is a trade-off in terms of visibility and proton dose perturbation, any type of marker system used should undergo dosimetric and visualization checks.[114–118]

An essential task of planar IG commissioning is to verify its image orientation correctness through the chain. The coordinate systems can vary between the planning, delivery, IG, and treatment management systems. Although usually confirmed earlier as part of the facility integration software-connectivity testing during end-to-end acceptance testing, it is recommended that the correct display of coordinate-based image data be verified as part of the IG commissioning. It is recommended that all clinical geometries intended for use have their IG process and correctness verified. Examples include verifications of different patient orientations, such as prone/supine and feet-first or head-first. Special care must be taken when using unusual patient positions, unusual gantry or couch angles, or a treatment chair. The image geometry correctness should be verified for potential up–down, left–-right, and mirroring errors. Once the planar IG system is processing and displaying information correctly, the registration process should be tested. For this purpose, a phantom may be intentionally translated and rotated away from its reference position. After that, the IG system should accurately indicate the displacement. During commissioning, it is especially important to perform this verification over the range of translations and rotations to be used clinically. Specifically, small translations of 1–3 mm, isocentric rotations, and more substantial translations associated with field junctions should be verified and their uncertainties incorporated into the clinical process. The planar IG system can be used to correct for couch sag relative to the planned geometry. The couch-sag behavior needs to be understood under various loading and orientation conditions to produce clinical use guidelines for the IG process.

The non–proton-specific extensive IG tests required for commissioning and are also used with other teletherapy modalities can be found in existing photon beam quality assurance reports.[119,120] These reports provide information about tolerances for quality assurance and control, including kilovoltages, mAs, low- and high-contrast resolution with different phantoms, and radiography tests. The dose associated with clinical imaging techniques must be determined, especially for pediatric cases. For any imaging system, the isocenter congruence should be re-verified (after acceptance testing), particularly in comparison to the proton isocenter and the mechanical isocenter.[121,122]

### 7.B. Volumetric image guidance

Volumetric IG offers the possibility of soft tissue as well as bony alignment. Additionally, the volumetric images might be used for dose recalculation[123–125] or adaptive purposes.[126] These functionalities are driving the integration of volumetric IG via cone-beam CT (CBCT) or CT on rails. The CT-on-rails systems can be placed inside[127,128] or outside[128] the treatment room. Volumetric IG can be combined with planar IG through the generation of DRRs. Commissioning CT-based IG systems for radiotherapy is discussed in detail in AAPM TG-179[129] and the previous TG-104 report.[120] Volumetric IG geometric accuracy tests should be completed as part of acceptance testing. Because of the dynamic nature of volumetric image-acquisition systems, the geometric accuracy should be evaluated compared to static planar systems. Hence, re-verification (post–acceptance testing) of the geometric and image accuracy should be performed during commissioning using the volumetric tools listed in Table III. The dynamic nature of CBCT systems also contributes to the risk of physical injury, especially in proximity to the nozzle, and more so with the use of a movable accessory mount. Collision detection and avoidance systems can reduce the motion injury and PTS damage risks, and if available, should be verified as part of acceptance testing.

It is crucial to commission the volumetric IG system for clinical use cases. The field-of-view (FOV) or length-of-view limitations of the volumetric imaging system may determine the clinical range of use. For example, small FOV images may be suitable for isocenter/target alignment verification but inadequate for skin/outer tissue geometry changes that may cause additional range changes relative to the target/OAR. If imaging is to be performed away from the treatment location, then geometric accuracy verifications should be provided over the relatively long transfer distances.[128] This should also be performed for non-coplanar setups.

## 8. TREATMENT MANAGEMENT SYSTEM COMMISSIONING

### 8.A. Background

Treatment management systems play vital roles in modern radiation oncology.[130] Their primary functions are to record and verify patient treatments. It should be noted that, for some TMS systems, the proton version of the TMS can differ significantly from its photon counterpart, and specific tests should be designed to test these aspects. The TMS either shares a database with the TPS or has its database. When the databases are separate, the TMS communicates with the TPS by using DICOM-RT, an extension of DICOM with radiation therapy information objects established in the mid-1990s.[131] To support general ion-based treatment planning and delivery processes, Working Group 7 of the DICOM Standards

Committee added DICOM-RT-ION, including RT-ION Plan and RT Ion Beams Treatment Record, to DICOM in Supplement 102 in the mid-2000s.[132] Although vendors provide DICOM conformance statements for their products, these statements are not a guarantee of compatibility between various devices, and potential non-compliance should be addressed during acceptance testing. Integrating the Healthcare Enterprise in Radiation Oncology, an American Society for Therapeutic Radiology and Oncology initiative seeks to achieve better interoperability in a multi-vendor clinical environment through the coordinated use of established standards, such as DICOM and HL7.[133,134]

### 8.B. Commissioning

During commissioning, the TMS functionality should be verified concerning correct data transfer and recording. There are several aspects to this verification. First, it should be verified that the planned treatment fields are downloaded into the TMS with the reference images as part of a DICOM-RT-ION plan. Second, the treatment-field parameters communicated to the delivery system for interlock checking should be verified at the delivery system hardware level. If used, ancillary devices such as apertures/compensators and EAs should also be interlock verified based on the TMS. Such interlocks must be present. They should be validated in the therapy control system too, that is, the interlocks should be verified by both the therapy control and TMS. Additional examples are nozzle settings, gantry angles, and couch angles. General delivery system interlock parameters such as proton range (planned vs machine delivery setting) also need to be set in the TMS. The IG data recorded at delivery are contained in the RT Beams Treatment Record and should be uploaded into the TMS as part of the treatment record and offline review, if desired. The images' orientation should be verified in the TMS and should match the correct orientation in the previously validated IG system (Section 7). The treatment record that includes verification images (together with the applied relative couch offsets) should also be checked. The recording and subsequent recovery of partially delivered fields should be verified using the TMS. Finally, it is recommended that the entire TMS-related workflow of patient verification, barcode scans (if used), patient setup, treatment delivery, and dose/MU/beam geometry/overrides and partial delivery be verified. This verification should be completed before end-to-end testing (Section 12).

## 9. PROTON MACHINE ABSOLUTE DOSE CALIBRATION

PTS output calibration to absolute dose is a central clinical commissioning task. The new user is faced with how to implement the biological effectiveness (RBE) factor required for proton therapy and implementing the calibration protocol with decisions on the reference field and ionization chamber used. The needed details are presented in the following sections.

### 9.A. Radiobiological effectiveness factor

This report addresses only physical dose calibration. After physical dose calibration, an additional relative RBE factor is required. The currently accepted RBE factor is 1.1, but this represents only an average value.[135] The user is cautioned to ensure that the RBE factor is only applied at a single point (not twice) in the treatment workflow. The most common places to use the factor are in the TMS or the TPS. Applying the factor in the TPS has the advantage that the planner and the radiation oncologist are provided with dose distributions in terms of Gy (RBE).[136] Either way, a single approach should be selected and applied consistently within the institution. For additional detailed information on the selection and implications of the RBE factor.[5]

### 9.B. Calibration protocol

Absolute dose calibration methods have evolved and continue to evolve for proton therapy. Measurement with tissue-equivalent detectors, dose to tissue, Faraday cups, and calorimetry have historically been performed, and most recently, dose to water determined using an ionization chamber calibrated in a 60-Co beam,[137,138] have been included. It is currently recommended that reference dose calibration be performed according to the $N_{D,w,Q_0}$-based method of calibrated ionization dosimetry presented in TRS-398.[139] The ionization chamber should be calibrated by an Accredited Dosimetry Calibration Laboratory (ADCL). Optionally, it is possible to further reduce the dose calibration uncertainty by using calorimetry.[140–144]

### 9.C. Reference field and point of measurement

Critical user choices in the calibration process are the determination of the type and size of the reference field to be used and the selection of the measurement point within the reference field. The reference field could be either a broad-scanned series of closely spaced individual monoenergetic beamlets (referred to in this section as a pristine beam but sometimes termed a monolayer) or a spread-out Bragg peak (SOBP) delivery. SOBP calibration is predominant and usually employs a $10 \times 10 \times 10$ cm$^3$ cubic field at a selected depth. Typically, the cubic field placement in depth is chosen to be representative of the "average" treatment field range intended for the practice. Alternatively, when the calibration is performed in a monoenergetic pristine beam, the relatively flat plateau region is used. In this case, because of the ionization chamber–specific factors that depend on the measurement-point depth, depths of at least 1 cm in water are recommended. A uniform set of equally weighted spots is scanned for the single-energy (pristine) field and scanned monolayer deliveries. The scanned monolayer approach potentially introduces measurement uncertainty from the ionization chamber position concerning field ripple. For this reason, it is recommended to use a spot spacing that reduces the

field ripple to <1% in the vicinity of the measurement location.[145]

## 9.D. Ionization chamber choice and associated uncertainties

The choice of a suitable ionization chamber for the absolute dosimetry provides a sound basis for the task. This requires knowledge about the chosen absolute dosimetry protocol, the user's implementation of the protocol, and the beam properties of the system to be calibrated. This generally means selecting a suitable size and shape of the dosimeter or applying correction factors of potentially greater magnitude, with their corresponding uncertainties.

Three sources of ionization chamber uncertainty can be considered contributing to the total absolute dosimetry of the proton beam: 60-Co calibration uncertainty, long-term stability uncertainty, and the uncertainties arising from TRS-398 calibration of the proton beam using the specific ionization chamber type.

### 9.D.1. $^{60}$Co-ionization chamber calibration uncertainty

Uncertainty arises from the calibration of ionization chambers at an ADCL. When using an ADCL calibrated cylindrical ionization chamber with TRS-398, the dosimetric uncertainty reportedly results in a 1.7% dose uncertainty, whereas using an ADCL calibrated plane-parallel chamber results in a 2.1% dose uncertainty. The difference in the reported uncertainties results from the $^{60}$Co calibration of the ionization chambers in the standards laboratory reference $^{60}$Co beam.

### 9.D.2. Long-term ionization chamber stability uncertainty

Mechanical properties can contribute to the uncertainties, including the mounting of the central electrode. The long-term stability of cylindrical chambers has been observed to be better than that for plane-parallel chambers in electron beams, with the differences in relative calibration coefficients being typically less than 0.1% over 5 years, whereas 0.2–0.3% was found to be typical for the types of parallel-plate ionization chambers used for proton therapy dosimetry.[146]

### 9.D.3. Calibration ionization chamber choice and absolute dosimetry uncertainties

When using TRS-398 with a calibrated ionization chamber, it is reportedly possible to achieve a total absorbed dose uncertainty for ionization-based absorbed-dose determinations based on calibrated ionization chambers of 2.6%.[136] It is also good practice to perform the calibration dosimetry verification or cross-calibration with two independently calibrated ionization chambers to mitigate any systematic error between chamber calibration dates.

Two practical sources of measurement uncertainty can impact the desired uncertainty magnitude: the effective point of measurement and the ionic recombination.

Subjectively, small-diameter plane-parallel chambers have a distinct measurement point in proton beams, and the effective point of measurement accuracy is arguably improved compared to cylindrical ionization chambers. Objectively, it has been reported that following the TRS-398 recommendation of positioning the reference point of a cylindrical chamber at the reference depth can lead to a systematic underestimation of absorbed dose for monoenergetic beams, especially for lower energy proton beams. Considered to be a dose gradient effect resulting from the effective measurement point of cylindrical ionization chambers, it is less evident with use in SOBPs.[147]

In general, the instantaneous dose rate from IMPT systems can be relatively high as the narrow proton beamlet is scanned across an ionization chamber. High instantaneous dose rates can elevate ion recombination in the collecting gas, especially for larger volume chambers, including cylindrical chambers.[148] Therefore, care should be taken about recombination factors that depend on the ionization chamber size, bias, and dose rate. Specifically, higher recombination correction factors can be expected for larger-volume cylindrical chambers (Farmer chambers) with IMPT cyclotron- and synchrocyclotron- vs synchrotron-based beams. The combination of IMPT systems possessing higher instantaneous dose rates from high flux accelerators with small spot sizes further exacerbates and the ionic recombination effect with larger ionization chambers.[149] Indeed, higher instantaneous dose rates and smaller spot sizes are a growing trend in proton therapy.

Generally, and historically, Farmer-type cylindrical chambers were commonly used for absolute dosimetry protocols associated with the "double scattering era." But, because of the issues relating to uncertainties of their use for IMPT dosimetry, the usage trend has been and is expected to continue toward small volume parallel plate chambers in the absolute dosimetry role for IMPT. Specifically, in some cases of combined ionization chamber choice and PTS, the required correction's magnitude due to ionic recombination may exceed 1% in higher flux beams. It is recommended by this group not to exceed 1% correction for ionic recombination.

Ionic recombination must be characterized experimentally by the end-user, but contributing are the design, fabrication, and assembly of the central electrode. Deviations can result in low $E$ field strength in small portions of the sensitive volume. In a guarded plane-parallel ionization chamber, the sensitive volume has a uniform and strong $E$ field, which avoids or minimizes most of the recombination issues mentioned. They may be less susceptible to recombination in high-flux IMPT systems. Furthermore, it is essential to understand the dosimetry system recombination behavior with the specific PTS. It is possible to gain understanding by measuring the entire response curve with multiple voltages and graphing the results for extrapolation.[150,151] But for commissioning, the 2-

voltage determination of the recombination factor[152] is widely used, although its underlying assumptions have been challenged for high instantaneous dose rate systems.[153] Increased chamber bias (within the chamber-bias specification range) may also reduce recombination in some cases. Finally, polarity corrections must also be considered, but they are typically negligible in proton beams for plane-parallel chambers.[154,155]

In summary, the uncertainties associated with absorbed dose calibration of proton beams can be classified as intrinsic and practice dependent. The inherent uncertainties stem from the physical characteristics of the ionization chamber and its $^{60}$Co calibration. The principal practice dependent uncertainties are associated with the accuracy of the effective point of measurement and the corrections for ionic recombination in the ionization chamber with an applied electric field. For these reasons, this group's recommendation is to use a calibrated, guarded, plane-parallel chamber for IMPT absolute absorbed dose calibration.

### 9.E. Interfacility comparisons and remote auditing

Consistency in calibration accuracy among proton therapy centers is vital if their clinical outcomes are to be compared. In 2008, after earlier efforts to make such comparisons,[156–158] the IROC launched a program for proton center dose verification and monitoring that is now widely used.[159] The National Cancer Institute (NCI) mandates participation in the program by those proton therapy institutions wishing to participate in NCI-sponsored clinical trials. Indeed, the IROC credentialing program is a valuable resource, and it is recommended that its services form part of the proton therapy system commissioning effort. Specifically, it is recommended that the machine dose calibration for the reference field be confirmed through the IROC before the first patient treatment.

## 10. OUT-OF-FIELD DOSE FROM PROTON THERAPY

Physicians treating patients with radiation need to assess the patient's secondary cancer risk from doses delivered to normal tissues outside the primary treatment field.[160–166] Except for a new type of system, or significant system modification where the proton beam is partially blocked in the treatment room as an example, measurements for out-of-field dose characterization are not necessarily required for clinical commissioning. However, it is recommended that the clinical staff be aware of the out-of-field dose magnitudes and distribution for their system. The following serves as an overview of the topic.

The out-of-field dose can originate from within the patient or from the radiation head (i.e., from stray radiation), the accelerator, or the energy selection system, depending on the amount of shielding provided. Generally, stray radiation (including that of neutrons) is a consideration in beamline design.[167] The latest IMPT scanning systems provide lower out-of-field doses than previous PTSs.[168,169] The planners and oncologists should be aware of these results as part of the clinical treatment planning process. But it is too complex and time-consuming to assess stray radiation exposures as part of routine clinical treatment planning. If desired, specific tests can be performed to evaluate out-of-field dose values.[170] Also, Moyers et al. have described various measurements that can be made for this purpose.[171] The subject of the out-of-field dose is also related to the treatment of pregnant patients and patients with implanted cardiac pacemakers and defibrillators. Published data on the comparative out-of-field dose from proton therapy are helpful for the assessment,[168,172–175] and the management of proton therapy patients with implanted cardiac pacemakers and defibrillators is specifically addressed in TG-203.[176]

## 11. RADIOTHERAPY PLANNING SYSTEM COMMISSIONING

This section on IMPT TPS commissioning includes a description of the most common type of IMPT dose model (provided to promote basic understanding), the specific measurements required to form the dose model, and different special features of IMPT systems and their applications. Because MC methods are expanding in use, they are also discussed.

IMPT systems, in contrast to previous types, use a building block approach to form their field. The building blocks are the individual "beamlets." Therefore, much of the effort in IMPT commissioning is in measuring and characterizing the beamlets for the complete range of energies and any beam modifying devices employed. The other elements of IMPT dose models and measurements are the energy settings, virtual source-to-axis distance, and effective source-to-axis distance, which are standard for radiotherapy machines. However, the fundamental difference in field generation results in some different uncertainties.[177] With the building-block approach, the concern is that relatively small errors under certain conditions may sum to larger errors during field delivery as the "blocks" sum together.

An example of this is the spot halo dose that, if unaccounted for, can lead to dose calculation errors more than 3%/3 mm for an excess percentage (>5%–10%) of points tested within fields.[178,179] This concern guides the commissioning effort to reduce errors in measurement and calculation as much as possible for the spot profiles and IDDs. With the resulting high-quality building-block data and dose model, IMPT commissioning should follow the generation and verification of uniform and non-uniform fields that are representative of the fields to be treated clinically.

MC methods are increasingly serving in two general areas: generation, verification, and correction of commissioning data needed as an input for the TPS dose model, and as a dose model directly internal or external to the TPS. Both applications are discussed here.

## 11.A. Dose modeling for treatment planning

### 11.A.1. Analytical dose model representation

Intensity modulated proton therapy dose modeling is typically performed using a pencil-beam algorithm. The elemental dose to a point from a proton pencil beam centered at $(x_0, y_0)$ can be expressed as

$$D_{PB}(x,y,z) = C(z_{eq}, x_0, y_0) \times O(z_{eq}, x - x_0, y - y_0), \quad (1)$$

where $z_{eq}$ is the water-equivalent depth of the pencil beam evaluated at the plane of calculation. The central-axis term C represents the depth dose, and the off-axis term O models the radial spread. The total dose for each point inside the calculation volume is computed by adding all the pencils' contributions within the beam.

The spot fluence profile can generally be modeled by a single Gaussian, with $\sigma_x$ and $\sigma_y$ characterizing the x- and y-distributions, respectively. The spot sizes (x and y) are plotted against the beam axis (z) and fitted to the following function[180]:

$$f(z) = \sqrt{\frac{A}{2} + B \cdot z + \frac{C}{2} \cdot z^2}, \quad (2)$$

where A, B, and C are the free-fitting phase space parameters used to model the beam propagation, and $\frac{A}{2}$ represents the variance ($\sigma^2$) values of the spots. The sigma values tend to vary with the gantry angles (typically within 5%), but TPSs may not model such dependency. In such a case, the average values from the measurements are used.[178] Beam spot shapes can deviate from the ideal Gaussian form, primarily because the multiple Coulomb scattering proximal to the nozzle exit is dependent on system design choices such as beam optics, accelerator properties, and scattering devices such as monitors. In contrast, the MCS distal to the nozzle is due to the effect of beam-modifying devices. To adequately model the in-air fluence in this situation, multiple Gaussian modeling has been introduced.[178,181]

### 11.A.2. Modeling low-dose Halo

Large-angle scattering and secondary products from nuclear interactions in water result in a low-dose halo centered on the narrow proton pencil beam. In some cases, this low-dose envelope can extend to a radius of up to 10 cm, and radial contributions from many neighboring pencils within a scanned beam can add up significantly. As much as 15% of the dose can be attributed to the beam halo.[179] This effect was not modeled in early scanning-beam algorithms. The most noticeable consequence is a systematic dependence of the observed dose as a function of the size of the target volume. Pedroni et al. proposed modeling the beam halo by using the following empirical formula[179]:

$$\begin{aligned} D(x,y,w) &= T(w) \times (1 - f_{NI}(w)) \times G_2^P(x, y, \sigma_p(w)) \\ &\quad + f_{NI}(w) \times G_2^{NI}(x, y, \sigma_{NI}(w)), \end{aligned} \quad (3)$$

where $D(x,y,w)$ represents the dose at a point in water at a depth w; $T(w)$ is the integral dose at depth w;$f_{NI}(w)$ is the fractional contribution at depth that is assigned to the nuclear interactions; and $G_2^P(x, y, \sigma_p(w))$ and $G_2^{NI}(x, y, \sigma_{NI}(w))$ are the two-dimensional Gaussian functions for the undisturbed primary beam and the low-dose envelope distributions, respectively.

### 11.A.3. Accuracy and limitations of analytical dose algorithms

Analytic dose algorithms (ADCs), commonly known as pencil beam algorithms,[180,182,183] are widely used for proton therapy treatment planning. Clinical implementation of ADCs is often optimized for speed rather than accuracy to achieve a reasonable calculation time. Users, therefore, should review and evaluate the accuracy specific to their clinical needs. For efficiency, Schaffner et al[180] uses an in-air fluence based calculation model. In the presence of a compensator, the perturbed fluence distribution due to scattering is accounted for according to the thickness profile. Changes in the energy distribution of the scattered protons, however, are ignored. This approximation can lead to significant errors near the vicinity of a sharp gradient, especially towards the end of the proton range. Analytic dose algorithms typically project the range based on the water equivalent depth in the patient to estimate the lateral spread at a given depth, ignoring the relative position of the inhomogeneities to the Bragg peak. For complex geometries and density variations such as at bone-soft tissue interfaces, ADC, given its limited ability in modeling multiple-Coulomb scattering, often fails to correctly predict the effects of range degradations and widening of the distal fall-off. These observations are evident in comparative studies using MC simulations.[184,185] Underestimation of doses to critical structure distal to the target, especially in low-density regions, has also been shown.[186] The range uncertainties in the calculation and the impact on dose accuracy are site-specific. In a study on five clinical sites, ADC was found to overestimate the tumor dose by 1–2% on average.[187] For complex geometries such as in head and neck and lung, approximations in ADC and its limited ability in modeling multiple-Coulomb scattering can lead to geometric miss from overestimating the range or predicting unrealistic dose homogeneity caused by underestimation or overestimation of scatting effects in tissue. For these clinical sites, advanced methods, such as MC simulations, can be beneficial.[188] MC calculations are also preferred over ADCs for dose calculations with IMPT systems degrading energy in the nozzle.

### 11.A.4. Monte Carlo as a dose model for treatment planning

Recently, several commercial TPSs have released MC dose calculation algorithms for IMPT. Due to their potentially increased accuracy over analytical algorithms,[189–191] the use

of MC dose calculations is expected to increase in routine clinical practice. Also, as these implementations are dedicated for treatment planning purposes, they are significantly faster than current general-purpose research codes, making their use in a clinical environment more attractive than before. In practice, MC calculations are most beneficial when calculating dose when beam-modifying devices such as EAs or apertures are used, and in planning cases involving inhomogeneities. Having the MC calculation available also enables exploratory calculations in addition to physical dose such as linear energy transfer and its variants. Finally, if a MC dose model is to be used clinically, it must be commissioned and verified. Verification can follow as with analytical algorithms (Section 11.F), including beam modifying devices and inhomogeneous materials. The MC dose model's verification is typically more straightforward in these particular situations because a closer agreement with physical measurements is easier to achieve than with more limited analytical algorithms.

### 11.B. Apertures and energy absorbers

Although IMPT usually operates without the need for physical beam modifying devices, the devices are sometimes needed. Most commonly, EAs, sometimes termed as range shifters, are used to produce lower (typically < 70 MeV) energies. Physical apertures are also coming into use for IMPT. Because the physical devices produce secondary scatter, their dose modeling is complicated. Accurate dose modeling of large-angle scattering in an IMPT beam from high-density beam modifiers is expected to require multiple Gaussian pencil-beam models[192] or MC simulations.

### 11.C. Dose normalization to absolute dose

Planning for IMPT requires *ab initio* physical dose correlation to absolute dosimetry (Gy/MU). This correlation can be accomplished by using parameterizations and an empirical model of the low-dose halo. A dose model based on first physical principles has been shown to predict the absolute dose delivered by the line-scanning system of the Paul Scherrer Institute.[179] The dose is normalized to the number of incident protons in the unit of Gy $mm^2$ per giga-proton. It can then be converted to Gy $mm^2$ per MU after calibrating the MUs using a standard protocol (Section 9). Note: the conversion of Gy $mm^2$ per giga-proton to Gy $mm^2$ per MU is energy-dependent. Given the total dose and each spot's relative weight in the plan, the MU for each spot can then be determined.[193] These developments form the basis for the current TPS calculated dose correlations to measured absolute dosimetry. The dose per MU is also affected by the presence of an EA. Fluence reduction from EA out-scatter should be evaluated with a series of Gy/MU measurements compared to the open field results.

### 11.D. Dose model data acquisition

For dose modeling, the TPS requires a set of beam measurements that are described in this section. Each type of measurement requires a specific set of equipment, as detailed in Table IV.

TABLE IV. Typical dose model measurements and methods for intensity-modulated proton therapy commissioning.

| Type | Modeling (M) calibration (C), or verification (V) | IMPT method and materials |
|---|---|---|
| Integral depth dose (IDD) with and without range shifter(s) | M | A large-diameter parallel-plate chamber scanned along a single central beamlet in a water phantom. Monte Carlo corrections are usually required for all current methods.[188] Although MLICs are useful for quality assurance, they are not recommended for IDD acquisition for the TPS modeling need |
| SOBP depth dose in water | C, V | Parallel-plate ionization chamber in a scanning water phantom. Change the setup geometry to each different SOBP center |
| Spot profiles X/Y with and without energy absorber(s) | M | Film or a scintillation detector. Measure across the energy band in multiple planes transverse to the central beamlet axis at, proximal to, and distal to the isocenter. The film and scintillation detector need to be validated for use in the scanning beam, avoiding saturation or quenching |
| Virtual source-to-axis distance [X] in air | M | Scanned proton-field film measurements. Defined as the physical magnet center. Verify with back-projection of in-air 50–50%radiation field widths along the central axis |
| Virtual source-to-axis distance [Y] in air | M | Same as above; VSAD(X) ≠ VSAD(Y) |
| Dose halo | M | Superposition measurements of an individual beamlet or peripheral scans around a central measurement point in air |
| Proton dose per MU density [Gy $mm^2$/MU] calibration per energy | C | A single monoenergetic fixed beamlet or scanned beamlets delivered to a large-diameter parallel-plate chamber or small-volume ionization chamber, respectively, fixed at a depth of 1–2 cm in a water phantom |
| Lateral dose profiles at depth | V | Scan at multiple depths Small-volume cylindrical ionization chamber in a scanning water phantom for integrated point measurements, or film, or scintillating detector. Change setup geometry to each different SOBP center. Measure at multiple depths |

### *11.D.1. Integral depth-dose measurement, scaling, and corrections*

Integral depth-dose (IDD) representation requires a multi-step process, including measurement, curve corrections, and dose scaling.

*Integral depth-dose measurement:* All of the system energies should have been verified as part of the acceptance testing. Commissioning of the TPS requires accurate measurement of a subset of these energies. For systems selecting their energy in or near the accelerator, the IDD scans are typically measured for model data input in 10 MeV steps. Systems degrading energy in the nozzle may rely on a single maximum energy IDD if the TPS adequately models the nozzle contained binary range degrader.[145,194] In this case, additional IDD verification measurements are needed (Section 11.F). Static, monoenergetic beamlets should be delivered for the IDD measurements. The IDD measurements should be performed with a large-diameter plane-parallel ionization chamber with its build-up values verified by the user.

Commercially available large-diameter ionization chambers have an active cross-section of 8.4–15 cm. A scanning water phantom with sub- millimetric positioning accuracy should be used. Geometrically, all the IDD scans should be performed at a fixed source-to-surface distance. The spacing of the measurement points in depth will be non-uniform. It is necessary to adjust the measurement step size to <1 mm to resolve the Bragg peak adequately.

*Integrated depth-dose curve corrections:* Depending on the system lateral beam dimension provided, the incident energy, and the depth of measurement, the ionization chamber area may or may not be sufficiently large to acquire the entire beamlet dose. MC simulations are commonly used to assess this situation and then correct the measured data if needed.[195] In practice, the magnitude of the required correction depends on the system spot size and the diameter of the plane-parallel chamber used to collect the IDD curve data. A generic example of the relationship for a 4 mm–beam sigma system correction factor with varying chamber diameter is shown in Fig. 2. Specific examples can be found in the literature.[196,197] Because only the plateau portion of the pristine Bragg curve requires correction, it may be easier to substitute the MC-derived curves once they have been normalized to measured peak values. The scaling of measured data by a calculated specific correction factor has also been reported.[178]

After calibrating MC-generated IDDs measured data, they may be preferred as the commissioning data inputs for the TPS because of the improved accuracy and smoothness of the data compared to specific physical measurements.[4,178]

*Integrated depth-dose scaling:* Because IDDs are relative measurements, they should be scaled for each energy as a function of the MUs (Fig. 3) or the number of protons, usually in $10^6$ or $10^9$ quanta, million protons (Mp), and giga-protons (Gp), respectively, according to the TPS requirements.

There are two approaches to scaling: one using a large-diameter plane-parallel ionization chamber with static, monoenergetic pristine beamlets; the other using a Farmer chamber with scanned, monoenergetic pristine fields (monolayers). According to the Fano theorem, the two approaches should give equivalent results.[198] In either case, the ionization chamber used should be ADCL calibrated or cross-calibrated to an ADCL calibrated chamber in a wide, flat, photon or proton field. It is recommended that the scaling measurements be performed at shallow depth in a water phantom. Water measurement depths of 1–2 cm are suggested so that (a) the entire energy range can be covered at a single physical position, and (b) low-energy secondary protons (and stray radiation) contribute to a limited degree. Because non-primary radiation is dependent on the delivery system, it is suggested that MC modeling can be used to characterize this radiation and guide the choice of measurement depth. The

Ratio of the dose for 40 cm detector to a detector of a given size

| d, Detector diameter, cm | D40/Dd |
|---|---|
| 2 | 0.67 |
| 4 | 1.02 |
| 6 | 1.07 |
| 8 | 1.06 |
| 10 | 1.05 |
| 12 | 1.03 |
| 14 | 1.02 |
| 16 | 1.02 |
| 18 | 1.01 |
| 20 | 1.01 |
| 22 | 1.00 |
| 24 | 1.00 |
| 32 | 1.00 |
| 36 | 1.00 |
| 40 | 1.00 |

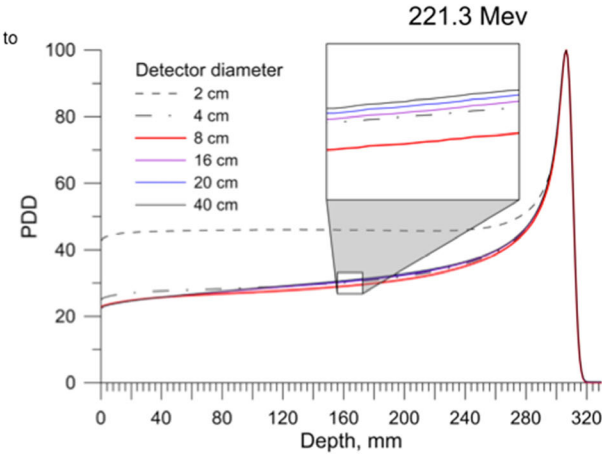


FIG. 2. Monte Carlo–determined missing halo dose percent depth-dose (PDD) correction factors at 10-cm water depth for a generic 4-mm spot sigma in air at 221 MeV as a function of the plane-parallel chamber integrating diameter. [Color figure can be viewed at wileyonlinelibrary.com]

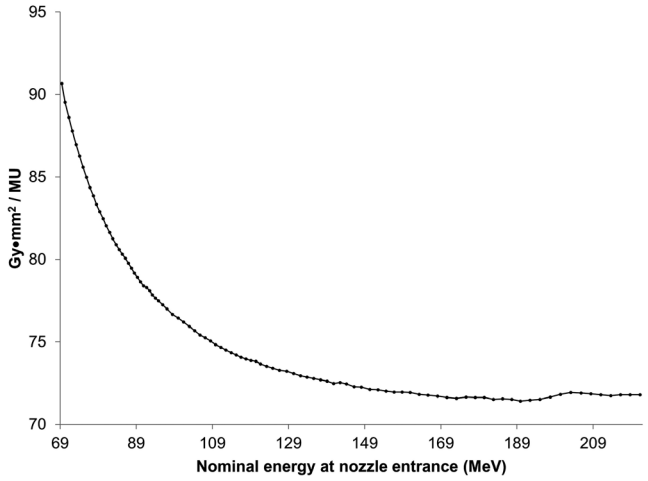


FIG. 3. Measured relation between dose and machine monitor units for 96 energies from a synchrotron-based proton therapy system. The measurements were performed at a constant depth of 2 cm in a water phantom using an 8.4-cm diameter calibrated ionization chamber (Bragg Peak chamber, PTW, Freiburg, Germany). The 96 data points correspond to individual synchrotron "energy tunes"; cyclotron-produced data would appear smoother as a result of continuous energy selection. [Color figure can be viewed at wileyonlinelibrary.com]

modeling goal is to determine the optimal measurement point where beam delivery induced low-energy secondary protons are stopped ahead of the detector while minimizing the amount of high angle MCS protons in the phantom proximal to the detector. Practically, this is within the range of 1–4 cm, and most typically 1–2 cm. After completion of these steps, the IDDs may be imported into the TPS for modeling.

### 11.D.2. Spot profiles

It is recommended that the lateral fluence distribution of the central-axis beam spot in air should be measured in the isocenter plane and at several distances proximal and distal to the isocenter plane along the beam axis (e.g., at ±10 and ±20 cm). It should also be evaluated in various radial directions to characterize the circularity of the spots and the gantry-angle dependency of the spot axes. The user should be aware that low-level spot fluence ("halo") extends far away from the spot axis. Consideration should be given to this aspect. Following the "building block" analogy (Section 11), the small components of spot fluence may sum to be significant for fields containing a high number of spots, depending on the magnitude of the tails. A superposition technique is usually applied because the halo portion of a spot fluence has a very low magnitude, practically 1/1000 of the maximum central beamlet value. By pairing measurements in superposition, one with a lower delivery magnitude for the central portion and the other with a higher delivery magnitude for the peripheral (halo) portion, the combined measurement's dynamic range can be extended as necessary. Both multi-element detectors and film have been used in this manner.[179,199–201] Spot halo analysis requires logarithmic plotting to observe the tails. The spot profiles serve as inputs for the dose algorithm. As discussed in Section 11.A.2, spot halos can affect the dose calculation accuracy. After dose modeling with the TPS, verification (Section 11.F) is needed. Should adjustment to the dose model be required, the spot halo contributions should be re-evaluated and adjusted if necessary.[178,202]

### 11.D.3. Virtual source-to-axis distance

With IMPT systems, there are usually two VSADs, one for each scanning direction [VSAD(X) and VSAD(Y)]. Usually, the VSADs can be assumed to be the distances from the respective scanning magnets' centers. The vendor will supply these values. The VSAD(s) of the magnet centers should be verified using individual scanned, monoenergetic pristine fields (monolayers) delivered at low, medium, and high system energies with in-air back-projection film or scintillation detector irradiations at several positions along and perpendicular to the central beam axis of 50–50% radiation field widths.[203]

### 11.D.4. Energy absorbers

The function of an EA is to reduce the range of the protons passing through it. This functionality is needed for treatments that require lower energies. Because EAs are a significant scattering source, an additional set of spot profile and IDD measurements are necessary for the TPS data modeling.

### 11.D.5. Ripple filters

Introducing a ripple filter requires additional commissioning. In part, this is because ripple filters rely on a specified drift distance between the filter and the intended delivery point, usually the isocenter. The region in which the ripple filter effect is acceptable should be determined. Because the beam properties are modified by the filter, using one usually requires specifying an additional treatment machine in the TPS.[204] Like EA modeling, ripple-filter dose modeling is currently being improved in commercial TPSs.

### 11.D.6. Apertures

The use of an aperture can reduce the penumbra from IMPT systems with larger spot sizes or when an EA is used.[205–208] Apertures must be thick enough to stop the incident protons. Practically, apertures are indicated for use for lower energies, and the maximum energy allowed corresponding to the equivalent aperture thickness should be fixed. The use of an aperture increases the secondary particle (neutron) out of field dose, and the amount should be known. Dose modeling when including beam scatter producing devices and combinations of beam scatter producing devices such as apertures, and EAs is more challenging than for "pure" scanning. Therefore, the TPS must be evaluated for suitability for purpose. High-performance analytical dose

algorithms[207] or MC dose algorithms[208] are usually required. In-air penumbra data is needed for analytical dose modeling, typically using a half beam block or field edge measurements.[207] Film or a scintillating detector should be used to measure the penumbra at the isocenter and several proximal and distal planes at distances ranging from −20 to +20 cm from the isocentric plane. Alternatively, a pinpoint ionization chamber may be used.[207] Depending on the clearance with the aperture mounted, the proximal plane distances may be reduced to accommodate the geometry. The penumbra measurements should be performed over the range of energies to be used with the apertures at maximum of 30 MeV intervals. It is recommended that after dose modeling, the model is validated using a mix of rectilinear and patient fields.[207] The validation should be performed at multiple depths (usually two or three) in water for each field.

### 11.E. Monitor unit determination

The IMPT inverse planning from the TPS should directly optimize the dose and associated MUs. Some centers specify treatment plans regarding the number of protons rather than MUs.[193] The resulting optimized plan is programmed directly into the proton therapy system for delivery. Hence, the TPS requires modeling the machine-dependent number of protons, Mp, Gp, or MU factors, such as energy, and the dependency on any beam-modifying device, such as the range shifter or an aperture.

For commercial TPSs, if necessary, users can generally incorporate dose-correction factors in the form of a dose-normalization table, typically a function of the beam energy or additional parameters such as the modulation width for uniform fields. Zhu et al. published a detailed report on commissioning a commercial planning system for pencil-beam scanning.[178]

### 11.F. Beam model verification

The beam modeling and TPS model verification is an iterative process. Through sequences of modeling, verification, and remodeling, if needed, the dose model and measurement should be brought to within an agreement of 2 mm/2% 98% for uniform fields in homogeneous media. Usually, one begins with the chosen reference field. The verification continues by investigating simple uniform fields of varying cubic dimensions at different depths, with and without beam-modifying devices. As examples, Table V presents some possible rectilinear field for dose model verification and, Fig. 4 shows a comparison of a few rectilinear field TPS dose calculations compared with ionization chamber measurements.

If repainting is employed, the simple uniform fields should be evaluated with it as well. The beam model should also be verified for any beam-modifying devices used. In the case of EAs, the spot size and penumbra width should be measured as a function of the air gap and beam configuration with the EA, and the TPS should accurately model the observed trend. IMPT systems degrading energy in the nozzle are a particular case of a binary EA system.[194] The verification of the beam model across the range of absorber function is recommended. The final verification proceeds with preclinical, patient-specific QA field deliveries.[178] It is recommended that the passing criteria for inhomogeneous fields be 3%/3 mm, with 95% of the points passing.

TABLE V. Possible rectilinear fields for TPS dose model verification.

| WET range [cm] | Modulation [cm] | Square fields [cm$^2$] | Oblong fields [cm$^2$] |
|---|---|---|---|
| 4 | 1, 2, 4 | 2, 5, 10, 20, max | 2 × 30, 4 × 30 |
| 6 | 3, 5 | 2, 5, 10, 20, max | 2 × 30, 4 × 30 |
| 8 | 4, 6, 8 | 2, 5, 10, 20, max | 2 × 30, 4 × 30 |
| 10 | 4, 6, 8 | 2, 5, 10, 20, max | |
| 12 | 6, 8, 10 | 2, 5, 10, 20, max | |
| 16 | 6, 8, 10 | 2, 5, 10, 20, max | |
| 20 | 6, 8, 10, 12 | 2, 5, 10, 20, max | 4 × 8 |
| 24 | 6, 8, 12 | 2, 5, 10, 20, max | |
| 28 | 6, 8, 10, 14 | 2, 5, 10, 20, max | 6 × 3 |
| 32 | 6, 8, 10, 15 | 2, 5, 10, 20, max | |

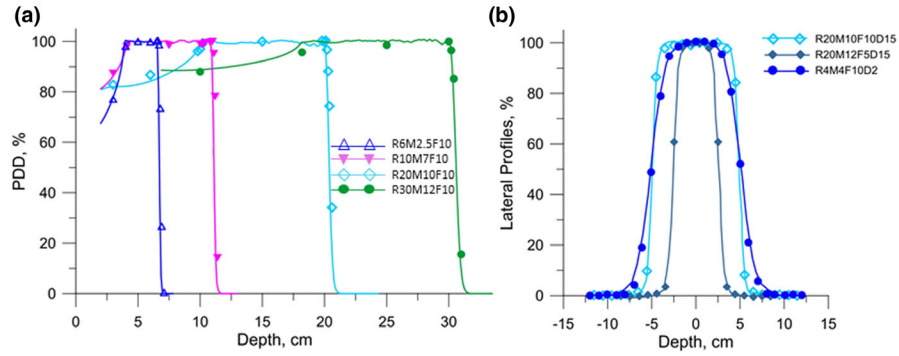


FIG. 4. Rectilinear verification fields from a synchrotron-based scanning system (a) longitudinal and (b) lateral comparing modeled dose distribution with ionization chamber measurements. The longitudinal comparisons are indicated by their SOBP widths, and the lateral comparisons are labeled according to their Range, Modulation width (SOBP), square Field size, and measurement Depth in x centimeters according to RxMxFxDx.

### 11.G. Role of Monte Carlo in data modeling

There are two situations in which MC simulations may be preferable to direct measurements: the first is when the total amount of data necessary to commission the system is such that opening the facility could be delayed because of the time needed to acquire the data, and the second is when limitations in the measurement make it difficult to obtain the necessary commissioning data. In either circumstance, the MC codes used need to be well understood and validated with measurements. The MC model is based on the physical devices and locations of the beamline components, most notably the nozzle, an example of which is presented in Fig. 5.

Most TPSs require integral depth-dose curves as input. Measuring these curves with a large-diameter ionization chamber and motorized water tank can be very time-consuming. Also, for large spot sizes, the commercially available ionization chambers may be too small to capture all the primary protons and secondary particles at all depths in the water tank. Figure 2 illustrates this point.

Because the design data are known well in advance of clinical operations, MC commissioning data can also be acquired well in advance. There are no practical limits on the detector size used in MC simulations in determining the integral dose. However, MC data are typically in units that are not easily converted to useful units for beam commissioning. Therefore, it is necessary to normalize the integral depth-dose curve with a single measurement obtained using a Bragg peak chamber at a suitable depth.[209] Because of the ionization chamber's finite size, this normalization may need to be corrected by modeling the ratio of the measured integral doses for the finite-size chamber and a large chamber[209] or by carefully measuring the beam profile at the normalization point.[195]

Similarly, planning systems require multiple spot profiles along both the major and minor axes of the beam spot, which can be elliptical.[209] Depending on the TPS, these profiles may be in water or air. The low-dose part of the spot dose profiles is most easily resolved by using MC simulations.[210]

## 12. END-TO-END VERIFICATION

Due to the complexity of IMPT systems and their internal interactions and dependencies, it is recommended that end-to-end verification must be performed before the onset of patient treatments. It is also recommended that the end-to-end verification should be performed for the typical clinical treatment sites representing the intended practice.

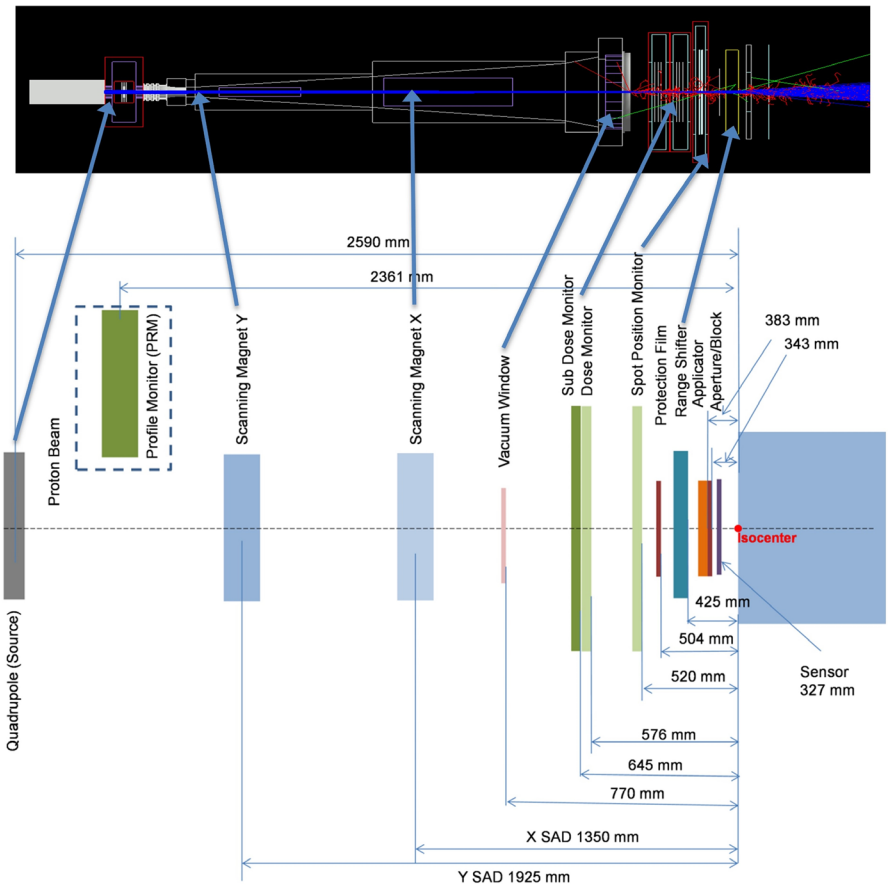


FIG. 5. Schematic layout (bottom) of a scanning nozzle showing physical dimensions used for modeling and the scale model representation used for calculation (top).[4] [Color figure can be viewed at wileyonlinelibrary.com]

TABLE VI. Test cases.

| Case type | Conditions | Field orientations | Test intent |
|---|---|---|---|
| Brain tumor | 3 fields, 2 Gy per fraction | 1 lateral, 2 non-coplanar | High-accuracy positioning |
| Upper abdomen/small lung tumor | 2 fields, 2 Gy per fraction, ~0.5-liter PTV | 1 lateral, 1 anterior | Target motion/gating |
| Sarcoma | 2 fields, 2 Gy per fraction, ~2.5-liter PTV | 1 lateral, 1 oblique | Large-field penumbra, delivery time dose uniformity, shallow dose, surface dose |
| Large lung tumor | 3 fields, 2 Gy per fraction, ~1.5-liter PTV | 1 anterior, 1 posterior, 1 oblique | Large-target dose uniformity, Under-couch beam clearance |
| Localized prostate cancer | 2 fields, 3 Gy per fraction, ~0.5-liter PTV | 2 lateral or lateral oblique fields | Deep-seated target, penumbra at depth |
| Craniospinal tumor | 3–4 fields, 2 Gy per fraction, ~1 to 1.5-liter PTV | 2 coplanar +2 posterior fields, all fields matched | Multifield setup, image guidance, field matching at depth |

### 12.A. Scope of end-to-end verification

The initial end-to-end testing should include the following: a simple phantom with slabs of water-equivalent plastic, low- and high-Z materials with known range-loss properties, and a simple target accommodating an ionization chamber. The water equivalent slabs should be evaluated for their expected range loss using a water phantom prior to use.[66] Commercially available options are available.[211] Subsequently, more advanced phantoms and dosimetry techniques can be used. End-to-end testing serves the following needs: TPS/TMS/TDS interface testing, PPS testing, dose distribution alignment with the IG system, patient-specific device fabrication, associated quality assurance, and staff training. Table VI lists a set of possible test cases designed to test planning and delivery system limits.

### 12.B. End-to-end testing methods and materials

Phantoms can be acquired to test these cases,[212,213] or clinical treatment fields may be planned based on a patient's CT data set and recomputed in a homogeneous water phantom before the clinical treatment fields are delivered to the phantom and measured. Anthropomorphic phantoms are to be preferred because they mimic human treatment better and provide a more realistic training component for the staff. They may also be more representative of geometric conditions, such as air gaps. The phantom-based method should be used whenever the facility adds new types of significantly different anatomical clinical targets.

After the beamlines (or delivery system), TPS, CT simulator, TMS, and patient imaging and alignment system have all been verified, the next step is to test the simulation, treatment planning, and delivery process's integrated functionality by performing end-to-end testing with a suitable phantom.

There should be space in the phantom to insert suitable dosimeters, such as TLDs, ion chambers, or film. Again, some dosimeters have a LET dependence, and the physicist should be aware of these. It is also necessary to have accurate knowledge of the proton-relative RLSP of the phantom's various materials in the irradiation field. The IROC has several mailable phantoms suitable for dose verification for targets in the prostate, lung, liver, brain, and spine. Commercially available phantoms can also be used for end-to-end testing. A dynamic or moving phantom should also be used to test the accuracy of the motion-management techniques used to treat moving targets.

After acquiring the CT images of the phantom and transferring them to the TPS, the validity of the CTN to RLSP conversion should be checked before treatment planning. The WETs of selected regions containing different materials can be obtained in the TPS and should be compared with the measured values. A suitable treatment plan should then be created in the TPS and put through the institutional QA checks before it is transferred to the TMS. Depending on the system, planar or volumetric imaging data should be prepared for IG. If used in the plan, apertures and range compensators are fabricated and should also undergo a QA process.

The treatment plan should be delivered to the phantom-appropriate dosimeters after the pretreatment QA process has been satisfied. The phantom should be set up by using the IG system. The necessary couch shifts should be determined by the IG software and applied to position the target in the treatment position. If used, patient- and device-identification barcode readers should be included during this end-to-end test.

The treatment delivery in clinical treatment mode should proceed and be recorded in the TMS. The treatment control system log should be checked to ensure that the field beam parameters delivered agree with those planned. The measured point dose and 2D dose-distribution values should be compared with those from the treatment plan. They should meet a minimum criterion of 3%/3mm, with 95% of the points passing.

### 12.C. End-to-end testing details

Unique to modulated beam delivery is a large amount of data used to specify the energy, position, and MUs for each spot. The application of a control point has a variety of vendor interpretations. A control point describes which parameters of the treatment machine change during beam delivery. In IMPT, control points have been used to describe energy

TABLE VII. Potential errors in the commissioning process and their mitigations.

| Sub-system | Error type | Error source | Occurrence (O) | (O) justification | Severity (S) | (S) impact | lack of detectability (D) | (D) justification | risk priority number RPN = O * S * D | Error mitigation |
|---|---|---|---|---|---|---|---|---|---|---|
| CT calibration | Range calculation | CTN to RLSP agreement | 10 | CT calibration mismatches may occur more than 5% of the time | 10 | Beam over or undershoot could produce a toxicity (over) or not provide local control (under) | 2 | The error should be found during range verifications using scanned phantoms | 200 | The CTN to RLSP curve should be reviewed by IROC |
| Image guidance | Geometric positioning | Commissioning error | 10 | Geometric positioning errors commonly occur during commissioning | 10 | Mispositioning of patient relative to beam could over or under dose | 1 | Geometric errors are easily identified. | 100 | Verify radiation field and image guidance system orientation and alignment independently with the IROC credentialing service |
| In-patient tissue heterogeneities | Dose and range calculations | CTN limited range and dose calculation algorithm | 3 | Patient inhomogeneities factor into a limited number of cases and current dose algorithms handle most of them fairly well | 10 | Local over and under dose near heterogeneity and increased range uncertainty. | 1 | The possible errors are readily detectable and materials of high density are readily identifiable | 30 | See Section 6.C on high atomic number materials. Refer also to TG-202: Physical Uncertainties in the Planning and Delivery of Light Ion Beam Treatments |
| Radiotherapy planning system | Dose and range calculations | Dose modeling | 3 | Volumetric dose distribution calculation errors sometimes occur | 2 | The magnitude of the severity from modest (<5%) volumetric dose errors is low. | 6 | Because the error magnitude is low, it is difficult to detect | 36 | Perform extensive patient specific field verifications at many energies, depths and field sizes. Find the limitations of the dose calculation model |
| Clinical commissioning data acquisition | Range | Range measurement error | 2 | Range measurement errors occur seldom | 10 | Over or undershoot could produce a toxicity (over) or not provide local control (under) | 1 | Error is readily detectable if comparison is made | 20 | Achieve agreement between physical measurements in water, Monte Carlo modeling (if used), and published range tables to within 1 mm |
| | | | | | Severity (S) | (S) impact | lack of detect-ability (D) | (D) justification | risk priority number RPN = O * S * D | Error Mitigation |
| Clinical commissioning data acquisition | Dose | Dose calibration error | 2 | Dose calibration error is unlikely, but could occur | 10 | Over or underdose entire target | 8 | Difficult to detect without independent comparison | 160 | Calibration according to established protocols. Verify calibrated dose using IROC service |
| Clinical commissioning data acquisition | SOBP measurement error | Commissioning error | 2 | SOBP measurement errors occur seldom | 10 | Over or under modulation could produce a toxicity (over) or high dose in the target (under) | 8 | Difficult to detect without independent comparison | 160 | Verify a subset of commissioned SOBPs with IROC credentialing service |

TABLE VII. Continued.

| Sub-system | Error type | Error source | Occurrence (O) | (O) justification | Severity (S) | (S) impact | lack of detectability (D) | (D) justification | risk priority number RPN = O * S * D | Error mitigation |
|---|---|---|---|---|---|---|---|---|---|---|
| Clinical commissioning data acquisition | Integral depth dose measurement error | Commissioning error | 3 | IDD measurement errors occur seldom | 8 | Wrong profile or magnitude could produce an incorrect planning model | 2 | Readily detectable from dose model validation | 48 | Verify a subset of commissioned integral depth doses with IROC credentialing service. Correct with Monte Carlo as necessary |
| Clinical commissioning data acquisition | Spot characterization measurement error | Commissioning/ modeling error | 6 | Spot profile measurement errors can occur with medium frequency | 5 | The dose model is not highly sensitive to modest spot profile measurement errors | 8 | Difficult to detect without independent comparison | 240 | Fully characterize spot tails and dose halo with at least 2 methods, or 1 method + Monte Carlo |
| Entire system | Systemic | System integration | 8 | Process errors are often identified in end-to-end testing | 10 | Could result in patient mistreatment | 8 | Difficult to detect without testing system as a whole | 640 | Perform end-to-end tests in "treatment mode" and quantitatively verify asymmetric field alignment and dose in phantom |

layers or transition points within energy layers. Some TPS and proton therapy control systems may have specific requirements, such as zero-weighted spots, to terminate a control point or end of treatment field delivery.

Intensity modulated proton therapy–specific areas of interest for commissioning regarding the TMS are the maximum deliverable versus recordable MU and the minimum MU. Clinically, before patient treatment commences, it is good practice to test patient-specific fields in the QA mode of the TMS, with the TDS in the treatment mode. After the treatment is delivered, the number of MU, spots, and spot positions that were delivered are uploaded from the TDS to the TMS for record-keeping and verification.[209]

An essential feature of the TMS or TDS (system-specific) is its ability to recover and deliver the remaining treatment in the event of a failure of either the TDS or the TMS, as the entire spot pattern must be delivered to treat the target with the prescribed dose. This recovery ability should be tested, especially when there is a discrepancy between the TDS and TMS. One possible approach is to deliberately cause failures in both the delivery system and the TMS. After such a failure, the number of spots delivered should be verified. The number of remaining spots should be determined and then delivered. A three-film test procedure was described by Gillin et al.[209]

## 13. POSSIBLE COMMISSIONING ERRORS AND MITIGATIONS

During commissioning, any measurement deviation from expected values should be investigated. The data should be consistent with each other. It is recommended that commissioning data and results be compared to published values where these are available. It is further recommended that the IROC credential the commissioned system. These steps can help avoid a major error. Table VII lists possible proton therapy commissioning errors that should be addressed as part of the commissioning process.

## 14. SUMMARY OF RECOMMENDATIONS

Below in Table VIII are the significant recommendations of TG-185. The commissioning team should produce a clinical commissioning report covering all the technical topics presented here. The commissioning data and results should be archived in a secure location for later reference. Portions of the data serve as a baseline for machine-specific quality assurance, as outlined in the TG-224.[2]

[a)]Author to whom correspondence should be addressed. Electronic mail: jonathan.brent.farr@cern.ch.

## REFERENCES

1. Mohan R, Paganetti H. Appendix: nomenclature and terminology in proton therapy. In: Das I, Paganetti H, ed. *Principles and Practice of Proton Beam Therapy*. Madison, WI: Medical Physics Publishing, Inc.; 2015:819–828.

TABLE VIII. Major recommendations for proton therapy clinical commissioning.

| Section no. | Title | Recommendation |
|---|---|---|
| 4 | Education, training, and timing | It is recommended that the commissioning team members (team) receive training in proton therapy |
| 4 | Education, training, and timing | The team should receive didactic education on general proton therapy principles and practice |
| 4 | Education, training, and timing | It is recommended that the new proton beam user setup the TPS as early as possible for planning exercises |
| 4 | Education, training, and timing | The team should be trained by the vendor regarding the specific operation of their proton therapy equipment |
| 4 | Education, training, and timing | The team should be trained by the vendor on the dosimetry equipment and systems |
| 4 | Education, training, and timing | Before commissioning a proton therapy system, it is recommended that the user be fully aware of the limitations of sensor and detector use in proton therapy |
| 4 | Education, training, and timing | External review by experienced planners is recommended before a system is first used to treat a patient. The external analysis should be performed by a multidisciplinary team, including at least one radiation oncologist and one medical physicist with extensive experience in proton therapy planning. The reviewers should review and suggest improvements for the proposed proton treatment planning policies and procedures as well as a representative sample of treatment plans covering the intended sites for treatment |
| 5 | Commissioning a CT scanner for proton therapy planning | It is recommended that a CT scanner be commissioned as a radiotherapy simulation scanner (CT simulator) |
| 5 | Commissioning a CT scanner for proton therapy planning | It is recommended that X-ray CT number (CTN) to relative linear stopping power (RLSP) conversion functions should be determined in order to provide accurate proton plan optimization and dose calculations |
| 5 | Commissioning a CT scanner for proton therapy planning | A standard phantom should be used, and verification of the CTN-RLSP fit from the Imaging and Radiation Oncology Core (IROC) Houston Quality Assurance Center is recommended |
| 5 | Commissioning a CT scanner for proton therapy planning | It is recommended that the resulting conversion functions should be accurate to within $\pm 2\%$ for soft tissues with near unit density |
| 5 | Commissioning a CT scanner for proton therapy planning | It is recommended that a separate conversion function should be generated for each set of CT scanner parameters (protocols) with different kVp, scan field-of-view size, and reconstruction kernel |
| 5 | Commissioning a CT scanner for proton therapy planning | It is recommended that if a plastic phantom must be used to generate the conversion function, offsets should be applied to construct a real tissue function |
| 6 | Ancillary devices and materials | It is recommended that any time a foreign material is introduced into the proton beam, its beam path length change be accounted for |
| 6 | Ancillary devices and materials | It is recommended that the alignment, uniformity, and WET be determined for each tabletop that will be used for therapy |
| 6 | Ancillary devices and materials | A set of physical and radiologic tests should be carried out to ensure the uniformity of the treatment couches to be used |
| 6 | Ancillary devices and materials | Because the WET function is nonlinear and begins to vary greatly at high angles, such high angles of incidence are best avoided. Also, to be avoided are the couch edges |
| 6 | Ancillary devices and materials | It is recommended to override the density of high–atomic number materials by using a measured RLSP corresponding to the CTN from the CT-simulator calibration. |
| 6 | Ancillary devices and materials | When treating through high-density materials, single-field treatment plans should be avoided |
| 6 | Ancillary devices and materials | Monte Carlo dose modeling is suggested when treating through high-density materials. Based on the results of modeling, suitable margins and a suitable number of fields should be used to provide sufficient robustness against range uncertainty and dose shadow effects |
| 7 | Commissioning image guidance systems for proton therapy | It is recommended that the accuracy of the PPS and IG system, including the accuracy of isocentric motion, be verified by acceptance testing before clinical commissioning |
| 7 | Commissioning image guidance systems for proton therapy | A setup accuracy guideline range is recommended that is synchronized with the treatment plan margins and robustness |
| 7 | Commissioning image guidance systems for proton therapy | It is recommended that the correct display of coordinate-based image data be verified as part of the IG commissioning |
| 7 | Commissioning image guidance systems for proton therapy | It is recommended that all clinical geometries intended for use have their IG process and correctness verified. Examples include verifications of different patient orientations, such as prone/supine and feet-first or head-first |
| 7 | Commissioning image guidance systems for proton therapy | The dose associated with clinical imaging techniques should be determined |
| 8 | Treatment management system commissioning | During commissioning, the TMS functionality should be validated concerning its correct data transfer and recording |
| 8 | Treatment management system commissioning | The recording and subsequent recovery of partially delivered fields should be verified using the TMS |
| 8 | Treatment management system commissioning | It is recommended that the entire TMS-related workflow of patient verification, barcode scans (if used), patient setup, treatment delivery, and dose/MU/beam geometry/overrides and partial delivery be verified |
| 9 | Proton machine absolute dose calibration | Reference dose calibration should be performed according to the Nw-based method of calibrated ionization dosimetry of TRS-398 |

TABLE VIII. Continued.

| Section no. | Title | Recommendation |
|---|---|---|
| 9 | Proton machine absolute dose calibration | The calibration for IMPT systems can be performed in either a pristine beam or a SOBP, but SOBP calibration is predominant |
| 9 | Proton machine absolute dose calibration | Care should be taken with regard to recombination factors that depend on the ionization chamber size, bias, and dose rate |
| 9 | Proton machine absolute dose calibration | It is recommended not to exceed 1% correction for ionic recombination |
| 9 | Proton machine absolute dose calibration | It is the recommendation to use a calibrated, guarded, parallel-plate chamber for the PTS absolute absorbed dose calibration |
| 9 | Proton machine absolute dose calibration | When the calibration is performed in a monoenergetic pristine beam, depths of at least 1 cm in water are recommended |
| 9 | Proton machine absolute dose calibration | When the calibration is performed using scanned monolayers, it is recommended to use a spot spacing that reduced the field ripple to <1% in the vicinity of the measurement location |
| 9 | Proton machine absolute dose calibration | It is recommended that the user conduct in-house uncertainty analyses for the absolute dose calibration |
| 9 | Proton machine absolute dose calibration | The machine dose calibration for the reference field should be confirmed through the IROC before the first patient treatment |
| 10 | Out-of-field Dose | It is recommended that the clinical staff be aware of the out-of-field dose magnitudes and distribution for their system |
| 11 | Radiotherapy planning system commissioning | Static, monoenergetic beamlets should be delivered for the IDD measurements. The IDD measurements should be performed with a large-diameter parallel-plate ionization chamber. The parallel-plate ionization chamber build-up values should be verified by the user. MLICs are not recommended for IDD acquisition |
| 11 | Radiotherapy planning system commissioning | The large-diameter ionization chamber should be calibrated or cross-calibrated to a calibrated chamber (Accredited Dosimetry Calibration Laboratory calibration) in a wide, flat, photon or proton field |
| 11 | Radiotherapy planning system commissioning | The IDDs should be scaled for each energy as a function of the monitor units or the number of particles, according to the requirements of the TPS |
| 11 | Radiotherapy planning system commissioning | It is recommended that the scaling measurements be performed at shallow depth in a water phantom. Water measurement depths of 1 to 2 cm are suggested |
| 11 | Radiotherapy planning system commissioning | A scanning water phantom with sub- millimetric positioning accuracy should be used |
| 11 | Radiotherapy planning system commissioning | Geometrically, all IDD scans should be performed at a fixed source-to-surface distance |
| 11 | Radiotherapy planning system commissioning | The IDD curves should be corrected for beam losses on the detector and scaled to dose or # protons per monitor chamber area |
| 11 | Radiotherapy planning system commissioning | It is recommended that the lateral fluence distribution of the central-axis beam spot in air be measured in the isocenter plane and at several distances proximal and distal to the isocenter plane along the beam axis (e.g., at $\pm$10 and $\pm$20 cm) |
| 11 | Radiotherapy planning system commissioning | Consideration should be given to the lateral fluence halo with measurement and modeling |
| 11 | Radiotherapy planning system commissioning | The VSAD(s) of the magnet centers should be verified using individual scanned, monoenergetic pristine fields (monolayers) delivered at low, medium, and high system energies, using in-air back-projection film exposures at several positions along and perpendicular to the central beam axis of 50–50% radiation field widths |
| 11 | Radiotherapy planning system commissioning | It is recommended that the dose model be validated using a mix of rectilinear and patient fields |
| 11 | Radiotherapy planning system commissioning | Through sequences of modeling, verification, and remodeling, if needed, the dose model and measurement should be brought to within agreement of 2 mm/2% 98% for uniform fields in homogeneous media |
| 11 | Radiotherapy planning system commissioning | IMPT systems degrading energy in the nozzle are a special case of a binary EA system. Verification of the beam model across the range of absorber function is recommended |
| 11 | Radiotherapy planning system commissioning | It is recommended that the passing criteria for inhomogeneous fields be 3%/3 mm, with 95% of the points passing |
| 12 | End-to-end verification | It is recommended that end-to-end verification must be performed prior to the onset of patient treatments |
| 12 | End-to-end verification | The measured point dose and 2D dose-distribution values should be compared with those from the treatment plan and should meet a minimum criterion of 3%/3mm, with 95% of the points passing. |
| 14 | Possible commissioning errors and mitigations | It is recommended that commissioning data and results be compared to published values where these are available |
| 14 | Possible commissioning errors and mitigations | It is recommended that the commissioned system be credentialed by the IROC |

2. Arjomandy B, Taylor P, Ainsley C, et al. *Report of the AAPM Task Group 224: Proton Machine QA*. College Park, MD: American Association of Physicists in Medicine; 2017.
3. Piersimoni P, Rimoldi A, Riccardi C, Pirola M, Molinelli S, Ciocca M. Optimization of a general-purpose, actively scanned proton beamline for ocular treatments: Geant4 simulations. *J Appl Clin Med Phys*. 2015;16:5227.
4. Farr JB, Moskvin V, Lukose RC, Tuomanen S, Tsiamas P, Yao W. Development, commissioning, and evaluation of a new intensity modulated minibeam proton therapy system. *Med Phys*. 2018;45 (9):4227–4237. https://doi.org/10.1002/mp.13093
5. Paganetti H, Blakely E, Carabe-Fernandez A, et al. Report of the AAPM TG-256 on the relative biological effectiveness of proton beams in radiation therapy. *Med Phys*. 2019;46:e53–e78.
6. Ciangaru G, Yang JN, Oliver PJ, et al. Verification procedure for isocentric alignment of proton beams. *J Appl Clin Med Phys*. 2007;8:65–75.
7. Farr JB, Dessy F, De Wilde O, Bietzer O, Schonenberg D. Fundamental radiological and geometric performance of two types of proton beam modulated discrete scanning systems. *Med Phys*. 2013;40:072101.
8. Smith A, Gillin M, Bues M, et al. The M. D. Anderson proton therapy system. *Med Phys*. 2009;36:4068–4083.
9. Farr JB, Kruse JJ. Acceptance testing. In: Das I, Paganetti H, ed. *Principles and Practice of Proton Beam Therapy.* Madison, WI: Medical Physics Publishing, Inc.; 2015:353–403.
10. Thomadsen B, Nath R, Bateman FB, et al. Potential hazard due to Induced radioactivity secondary to radiotherapy: the report of Task Group 136 of the American Association of Physicists in Medicine. *Health Phys*. 2014;107:442–460.
11. American College of Radiology (ACR). ACR–AAPM Technical standard for the performance of proton beam radiation therapy. Reston, VA; 2018.
12. Farr JB, Flanz JB, Gerbershagen A, Moyers MF. New horizons in particle therapy systems. *Med Phys*. 2018;45:e953–e983.
13. Farr JB, Maughan RL. Dosimetry for proton and carbon ion therapy. In: Ma C-M, Lomax AJ, eds. *Proton and Carbon Ion Therapy.* Boca Raton: CRC Press; 2013.
14. Palmans H. Dosimetry. In: Paganetti H, ed. *Proton Therapy Physics*. Boca Raton: CRC Press; 2013.
15. International Electrotechnical Commission (IEC). ISO: 14253-1:2013: Geometrical product specifications. Geneva; 2013.
16. International Electrotechnical Commission (IEC). Medical electrical equipment - Particular requirements for the basic safety and essential performance of light ion beam medical electrical equipment. Geneva; 2014.
17. Das IJ, Paganetti H. *Principles and Practice of Proton Beam Therapy.* Madison, WI: Medical Physics Publishing, Inc.; 2015.
18. Vatnitsky AS, Moyers MF. *Practical Implementation of Light Ion Beam Treatments*. Madison: Medical Physics Publishing; 2013.
19. Paganetti H. *Proton Therapy Physics*, 2nd edn. Boca Raton: CRC Press; 2018.
20. Ma C-M, Lomax AJ. *Proton and Carbon Ion Therapy.* Boca Raton: CRC Press; 2013.
21. Andreo B, Hohlfeld H, Kanai L, Smyth V. Absorbed Dose Determination in External Beam Radiotherapy: An International Code of Practice for Dosimetry based on Standards of Absorbed Dose to Water (Technical Report Series 398); 2004, Vienna.
22. Martisikova M, Jäkel O. Gafchromic (R) EBT films for ion dosimetry. *Radiat Measur.* 2010;45:1268–1270.
23. Mumot M, Mytsin GV, Molokanov AG, Malicki J. The comparison of doses measured by radiochromic films and semiconductor detector in a 175MeV proton beam. *Phys Med*. 2009;25:105–110.
24. Reinhardt S, Hillbrand M, Wilkens JJ, Assmann W. Comparison of Gafchromic EBT2 and EBT3 films for clinical photon and proton beams. *Med Phys*. 2012;39:5257–5262.
25. Niroomand-Rad A, Blackwell CR, Coursey BM, et al. Radiochromic film dosimetry: recommendations of AAPM Radiation Therapy Committee Task Group 55. American Association of Physicists in Medicine. *Med Phys*. 1998;25:2093–2115.
26. Vatnitsky SM. Radiochromic film dosimetry for clinical proton beams. *Appl Radiat Isot*. 1997;48:643–651.
27. Newhauser W, Fontenot J, Zheng YS, et al. Monte Carlo simulations for configuring and testing an analytical proton dose-calculation algorithm. *Phys Med Biol*. 2007;52:4569–4584.
28. Khatonabadi M, Zhang D, Mathieu K, et al. A comparison of methods to estimate organ doses in CT when utilizing approximations to the tube current modulation function. *Med Phys*. 2012;39:5212–5228.
29. Tian X, Li X, Segars WP, Frush DP, Samei E. Prospective estimation of organ dose in CT under tube current modulation. *Med Phys*. 2015;42:1575–1585.
30. Khatonabadi M, Kim HJ, Lu P, et al. The feasibility of a regional CTDI volume to estimate organ dose from tube current modulated CT exams. *Med Phys*. 2013;40:1–11.
31. Moore BM, Brady SL, Mirro AE, Kaufman RA. Size-specific dose estimate (SSDE) provides a simple method to calculate organ dose for pediatric CT examinations. *Med Phys*. 2014;41:1–9.
32. Turner AC, Zhang D, Khatonabadi M, et al. The feasibility of patient size-corrected, scanner-independent organ dose estimates for abdominal CT exams. *Med Phys*. 2011;38:820–829.
33. McCollough CH, Bakalyar DM, Bostani M, et al. Use of water equivalent diameter for calculating patient size and size-specific dose estimates (SSDE) in CT: report of AAPM Task Group 220. *AAPM Rep*. 2014;2014:6–23.
34. Moyers MF, Toth T, Sadagopan R, et al. Report No. 202 - Physical Uncertainties in the Planning and Delivery of Light Ion Beam Treatments. American Association of Physicists in Medicine; 2020.
35. Moyers MF, Sardesai M, Sun S, Miller DW. Ion stopping powers and CT numbers. *Med Dosim*. 2010;35:179–194.
36. Fippel M, Soukup M. A Monte Carlo dose calculation algorithm for proton therapy. *Med Phys*. 2004;31:2263–2273.
37. Schneider W, Bortfeld T, Schlegel W. Correlation between CT numbers and tissue parameters needed for Monte Carlo simulations of clinical dose distributions. *Phys Med Biol*. 2000;45:459–478.
38. Jiang HY, Seco J, Paganetti H. Effects of Hounsfield number conversion on CT based proton Monte Carlo dose calculations. *Med Phys*. 2007;34:1439–1449.
39. Kanematsu N, Matsufuji N, Kohno R, Minohara S, Kanai T. A CT calibration method based on the polybinary tissue model for radiotherapy treatment planning. *Phys Med Biol*. 2003;48:1053–1064.
40. Jiang H, Paganetti H. Adaptation of GEANT4 to Monte Carlo dose calculations based on CT data. *Med Phys*. 2004;31:2811–2818.
41. Battista JJ, Meeker B, Chapman D, Castor W. Animal tumor volume and density by CT. *J Comput Assisted Tomogr.* 1980;4:714.
42. Sontag MR, Battista JJ, Bronskill MJ, Cunningham JR. Implications of computed tomography for inhomogeneity corrections in photon beam dose calculations. *Radiology.* 1977;124(1):143–149.
43. Chen GTY. Quantitative CT in charged-particle radiotherapy. *J Comput Assisted Tomogr.* 1979;3:861–862.
44. Schneider U, Pedroni E, Lomax A. The calibration of CT Hounsfield units for radiotherapy treatment planning. *Phys Med Biol*. 1996;41:111–124.
45. Schaffner B, Pedroni E. The precision of proton range calculations in proton radiotherapy treatment planning: experimental verification of the relation between CT-HU and proton stopping power. *Phys Med Biol*. 1998;43:1579–1592.
46. Moyers M, Sun S, Sardesai M, et al. Tornotherapy MVXCT numbers versus RLSP for various ions and materials. *Med Phys*. 2007;34:2383.
47. Moyers MF. Comparison of x ray computed tomography number to proton relative linear stopping power conversion functions using a standard phantom. *Med Phys*. 2014;41:061705.
48. Taylor P, Lowenstein J, Kry S, Ibbott G, Followill D. A comparison of CT number to relative linear stopping power conversion curves used by proton therapy centers. *Med Phys*. 2015;42:3616.
49. Grant RL, Summers PA, Neihart JL, et al. Relative stopping power measurements to aid in the design of anthropomorphic phantoms for proton radiotherapy. *J Appl Clin Med Phys*. 2014;15:121–126.
50. Saito M. Spectral optimization for measuring electron density by the dual-energy computed tomography coupled with balanced filter method. *Med Phys*. 2009;36:3631–3642.
51. Bourque AE, Carrier JF, Bouchard H. A stoichiometric calibration method for dual energy computed tomography. *Phys Med Biol*. 2014;59:2059–2088.

52. Yang M, Virshup G, Clayton J, Zhu XR, Mohan R, Dong L. Theoretical variance analysis of single- and dual-energy computed tomography methods for calculating proton stopping power ratios of biological tissues. *Phys Med Biol*. 2010;55:1343–1362.
53. Han D, Siebers JV, Williamson JF. A linear, separable two-parameter model for dual energy CT imaging of proton stopping power computation. *Med Phys*. 2016;43:600–612.
54. Hünemohr N, Krauss B, Dinkel J, et al. Ion range estimation by using dual energy computed tomography. *Z Med Phys*. 2013;23:300–313.
55. Hünemohr N, Krauss B, Tremmel C, Ackermann B, Jakel O, Greilich S. Experimental verification of ion stopping power prediction from dual energy CT data in tissue surrogates. *Phys Med Biol*. 2014;59:83–96.
56. Yang M, Zhu XR, Park PC, et al. Comprehensive analysis of proton range uncertainties related to patient stopping-power-ratio estimation using the stoichiometric calibration. *Phys Med Biol*. 2012;57:4095–4115.
57. Liebl J, Paganetti H, Zhu M, Winey BA. The influence of patient positioning uncertainties in proton radiotherapy on proton range and dose distributions. *Med Phys*. 2014;41:091711.
58. Park PC, Cheung JP, Zhu XR, et al. Statistical assessment of proton treatment plans under setup and range uncertainties. *Int J Radiat Oncol Biol Phys*. 2013;86:1007–1013.
59. Kruse JJ. Immobilization and simulation. In: Das I, Paganetti H, eds. *Principles and Practice of Proton Beam Therapy*. Madison, WI: Medical Physics Publishing, Inc.; 2015:521–537.
60. Wroe AJ, Bush DA, Schulte RW, Slater JD. Clinical immobilization techniques for proton therapy. *Technol Cancer Res Treat*. 2015;14:71–79.
61. Wroe AJ, Bush DA, Slater JD. Immobilization considerations for proton radiation therapy. *Technol Cancer Res Treat*. 2014;13:217–226.
62. Wroe AJ, Ghebremedhin A, Gordon IR, Schulte RW, Slater JD. Water equivalent thickness analysis of immobilization devices for clinical implementation in proton therapy. *Technol Cancer Res Treat*. 2014;13:415–420.
63. Olch AJ, Gerig L, Li H, Mihaylov I, Morgan A. Dosimetric effects caused by couch tops and immobilization devices: report of AAPM Task Group 176. *Med Phys*. 2014;41.061501-1–061501-30.
64. Kim JS, Yoon M, Ahn S, et al. Modeling of a digital couch for a proton treatment planning system. *J Korean Phys Soc*. 2009;55:1640–1648.
65. Zhang R, Taddei PJ, Fitzek MM, Newhauser WD. Water equivalent thickness values of materials used in beams of protons, helium, carbon and iron ions. *Phys Med Biol*. 2010;55:2481–2493.
66. Zhang R, Newhauser WD. Calculation of water equivalent thickness of materials of arbitrary density, elemental composition and thickness in proton beam irradiation. *Phys Med Biol*. 2009;54:1383–1395.
67. Tatsuzaki H, Urie MM. Importance of precise positioning for proton beam therapy in the base of skull and cervical spine. *Int J Radiat Oncol Biol Phys*. 1991;21:757–765.
68. Fellin F, Righetto R, Fava G, Trevisan D, Amelio D, Farace P. Water equivalent thickness of immobilization devices in proton therapy planning - modelling at treatment planning and validation by measurements with a multi-layer ionization chamber. *Phys Med*. 2017;35:31–38.
69. Vargas C, Mahajan C, Fryer A, et al. Rectal dose-volume differences using proton radiotherapy and a rectal balloon or water alone for the treatment of prostate cancer. *Int J Radiat Oncol Biol Phys*. 2007;69:1110–1116.
70. Hedrick SG, Fagundes M, Robison B, et al. A comparison between hydrogel spacer and endorectal balloon: an analysis of intrafraction prostate motion during proton therapy. *J Appl Clin Med Phys*. 2017;18:106–112.
71. Newhauser WD, Giebeler A, Langen KM, Mirkovic D, Mohan R. Can megavoltage computed tomography reduce proton range uncertainties in treatment plans for patients with large metal implants? *Phys Med Biol*. 2008;53:2327–2344.
72. Wei JK, Sandison GA, Hsi WC, Ringor M, Lu XY. Dosimetric impact of a CT metal artefact suppression algorithm for proton, electron and photon therapies. *Phys Med Biol*. 2006;51:5183–5197.
73. Lee KYG, Cheng HMJ, Chu CY, Tam CWA, Kan WK. Metal artifact reduction by monoenergetic extrapolation of dual-energy CT in patients with metallic implants. *J Orthop Surg (Hong Kong)*. 2019;27:2309499019851176.
74. Liao E, Srinivasan A. Applications of dual-energy computed tomography for artifact reduction in the head, neck, and spine. *Neuroimaging Clin N Am*. 2017;27:489–497.
75. Nair JR, DeBlois F, Ong T, et al. Dual-energy CT: balance between iodine attenuation and artifact reduction for the evaluation of head and neck cancer. *J Comput Assist Tomogr*. 2017;41:931–936.
76. Paudel MR, Mackenzie M, Fallone BG, Rathee S. Evaluation of normalized metal artifact reduction (NMAR) in kVCT using MVCT prior images for radiotherapy treatment planning. *Med Phys*. 2013;40:081701.
77. Pessis E, Sverzut JM, Campagna R, Guerini H, Feydy A, Drape JL. Reduction of metal artifact with dual-energy CT: virtual monospectral imaging with fast kilovoltage switching and metal artifact reduction software. *Semin Musculoskelet Radiol*. 2015;19:446–455.
78. Landry G, Hua CH. Current state and future applications of radiological image guidance for particle therapy. *Med Phys*. 2018;45: e1086–e1095.
79. Koehler AM. Proton radiography. *Science*. 1968;160:303–304.
80. Koehler AM. Proton radiography. *Phys Med Biol*. 1970;15:181.
81. Schneider U, Pedroni E. Proton radiography as a tool for quality-control in proton therapy. *Med Phys*. 1995;22:353–363.
82. Pemler P, Besserer J, de Boer J, et al. A detector system for proton radiography on the gantry of the Paul-Scherrer-Institute. *Nucl Instrum Meth A*. 1999;432:483–495.
83. Sadrozinski HFW, Bashkirov V, Bruzzi M, et al. Issues in proton computed tomography. *Nucl Instrum Meth A*. 2003;511:275–281.
84. Sadrozinski HFW, Bashkirov V, Keeney B, et al. Toward proton computed tomography. *IEEE Trans Nucl Sci*. 2004;51:3–9.
85. Schneider U, Besserer J, Pemler P, et al. First proton radiography of an animal patient. *Med Phys*. 2004;31:1046–1051.
86. de Assis JT, Yevseyeva O, Evseev I, et al. Proton computed tomography as a tool for proton therapy planning: preliminary computer simulations and comparisons with x-ray CT basics. *X-Ray Spectrom*. 2005;34:481–492.
87. Schulte RW, Bashkirov V, Klock MCL, et al. Density resolution of proton computed tomography. *Med Phys*. 2005;32:1035–1046.
88. Talamonti C, Reggioli V, Bruzzi M, et al. Proton radiography for clinical applications. *Nucl Instrum Meth A*. 2010;612:571–575.
89. Esposito M, Waltham C, Taylor JT, et al. PRaVDA: the first solid-state system for proton computed tomography. *Phys Med*. 2018;55:149–154.
90. Schulte RW, Bashkirov V, Johnson R, Sadrozinski HF, Schubert KE. Overview of the LLUMC/UCSC/CSUSB phase 2 proton CT project. *Trans Am Nucl Soc*. 2012;106:59–62.
91. Knecht ML, Wang N, Vassantachart A, Mifflin R, Slater JD, Yang GY. Individualized 4-dimensional computed tomography proton treatment for pancreatic tumors. *J Gastrointest Oncol*. 2017;8:675–682.
92. Xie Y, Bentefour EH, Janssens G, et al. Prompt Gamma imaging for in vivo range verification of pencil beam scanning proton therapy. *Int J Radiat Oncol Biol Phys*. 2017;99:210–218.
93. Richter C, Pausch G, Barczyk S, et al. First clinical application of a prompt gamma based in vivo proton range verification system. *Radiother Oncol*. 2016;118:232–237.
94. Hueso-Gonzalez F, Fiedler F, Golnik C, et al. Compton camera and prompt gamma ray timing: two methods for in vivo range assessment in proton therapy. *Front Oncol*. 2016;6:80.
95. Verburg JM, Testa M, Seco J. Range verification of passively scattered proton beams using prompt gamma-ray detection. *Phys Med Biol*. 2015;60:1019–1029.
96. Polf JC, Avery S, Mackin DS, Beddar S. Imaging of prompt gamma rays emitted during delivery of clinical proton beams with a Compton camera: feasibility studies for range verification. *Phys Med Biol*. 2015;60:7085–7099.
97. Verburg JM, Seco J. Proton range verification through prompt gamma-ray spectroscopy. *Phys Med Biol*. 2014;59:7089–7106.
98. Polf JC, Mackin D, Lee E, Avery S, Beddar S. Detecting prompt gamma emission during proton therapy: the effects of detector size and distance from the patient. *Phys Med Biol*. 2014;59:2325–2340.

99. Golnik C, Hueso-Gonzalez F, Muller A, et al. Range assessment in particle therapy based on prompt gamma-ray timing measurements. *Phys Med Biol*. 2014;59:5399–5422.
100. Verburg JM, Riley K, Bortfeld T, Seco J. Energy- and time-resolved detection of prompt gamma-rays for proton range verification. *Phys Med Biol*. 2013;58:L37–L49.
101. Combs SE, Bauer J, Unholtz D, et al. Monitoring of patients treated with particle therapy using positron-emission-tomography (PET): the MIRANDA study. *BMC Cancer*. 2012;12:133.
102. Hsi WC, Indelicato DJ, Vargas C, Duvvuri S, Li Z, Palta J. In vivo verification of proton beam path by using post-treatment PET/CT imaging. *Med Phys*. 2009;36:4136–4146.
103. Meissner H, Fuchs H, Hirtl A, Reschl C, Stock M. Towards offline PET monitoring of proton therapy at MedAustron. *Z Med Phys*. 2019;29:59–65.
104. Moteabbed M, Espana S, Paganetti H. Monte Carlo patient study on the comparison of prompt gamma and PET imaging for range verification in proton therapy. *Phys Med Biol*. 2011;56:1063–1082.
105. Nishio T, Ogino T, Nomura K, Uchida H. Dose-volume delivery guided proton therapy using beam on-line PET system. *Med Phys*. 2006;33:4190–4197.
106. Oelfke U, Lam GK, Atkins MS. Proton dose monitoring with PET: quantitative studies in Lucite. *Phys Med Biol*. 1996;41:177–196.
107. Parodi K, Bortfeld T, Enghardt W, et al. PET imaging for treatment verification of ion therapy: Implementation and experience at GSI Darmstadt and MGH Boston. *Nucl Instrum Meth A*. 2008;591:282–286.
108. Parodi K, Enghardt W. Potential application of PET in quality assurance of proton therapy. *Phys Med Biol*. 2000;45:N151–N156.
109. Zhu XP, Espana S, Daartz J, et al. Monitoring proton radiation therapy with in-room PET imaging. *Phys Med Biol*. 2011;56:4041–4057.
110. Yoon M, Cheong M, Kim J, Shin DH, Park SY, Lee SB. Accuracy of an automatic patient-positioning system based on the correlation of two edge images in radiotherapy. *J Digit Imaging*. 2011;24:322–330.
111. Bennett KF, Ruther H, Vandervlugt G, Yates ADB. Patient positioning for proton therapy at the National-Accelerator-Center. *S Afr J Sci*. 1994;90:370–371.
112. Devicienti S, Strigari L, D'Andrea M, Benassi M, Dimiccoli V, Portaluri M. Patient positioning in the proton radiotherapy era. *J Exp Clin Canc Res*. 2010;29:47.
113. Grusell E, Montelius A, Russell KR, et al. Patient positioning for fractionated precision radiation treatment of targets in the head using fiducial markers. *Radiother Oncol*. 1994;33:68–72.
114. Habermehl D, Henkner K, Ecker S, Jäkel O, Debus J, Combs SE. Evaluation of different fiducial markers for image-guided radiotherapy and particle therapy. *J Radiat Res*. 2013;54:61–68.
115. Matsuura T, Maeda K, Sutherland K, et al. Biological effect of dose distortion by fiducial markers in spot-scanning proton therapy with a limited number of fields: A simulation study. *Med Phys*. 2012;39:5584–5591.
116. Newhauser W, Fontenot J, Koch N, et al. Monte Carlo simulations of the dosimetric impact of radiopaque fiducial markers for proton radiotherapy of the prostate. *Phys Med Biol*. 2007;52:2937–2952.
117. Newhauser WD, Koch NC, Fontenot JD, et al. Dosimetric impact of tantalum markers used in the treatment of uveal melanoma with proton beam therapy. *Phys Med Biol*. 2007;52:3979–3990.
118. Ramirez E, Zheng Y, Rana S. SU-E-J-33: proton therapy fiducial comparison. *Med Phys*. 2013;40:157.
119. Klein EE, Hanley J, Bayouth J, et al. Task Group 142 report: Quality assurance of medical accelerators. *Med Phys*. 2009;36:4197–4212.
120. Yin F, Wong J, et al. Report No. 104: the role of in-room kV x-ray imaging for patient setup and target localization. American Association of Physicists in Medicine; 2009.
121. Arjomandy B, Sahoo N, Zhu XR, et al. An overview of the comprehensive proton therapy machine quality assurance procedures implemented at The University of Texas M. D. Anderson Cancer Center Proton Therapy Center-Houston. *Med Phys*. 2009;36:2269–2282.
122. Newhauser WD, Hunjan S. Quality assurance of proton therapy. In: Pawlicki T, Dunscombe P, Mundt AJ, Scalliet P, ed. *Quality and Safety in Radiotherapy*. Boca Raton: CRC Press; 2011.
123. Zhang XD, Dong L, Lee AK, et al. Effect of anatomic motion on proton therapy dose distributions in prostate cancer treatment. *Int J Radiat Oncol Biol Phys*. 2007;67:620–629.
124. Landry G, Dedes G, Zollner C, et al. Phantom based evaluation of CT to CBCT image registration for proton therapy dose recalculation. *Phys Med Biol*. 2015;60:595–613.
125. Landry G, Nijhuis R, Dedes G, et al. Investigating CT to CBCT image registration for head and neck proton therapy as a tool for daily dose recalculation. *Med Phys*. 2015;42:1354–1366.
126. Chen WJ, Gemmel A, Rietzel E. A patient-specific planning target volume used in 'plan of the day' adaptation for interfractional motion mitigation. *J Radiat Res*. 2013;54:82–90.
127. Dong L, Cheung JP, Zhu XR. Image-guided proton and carbon ion therapy. In: Ma L, ed. *Proton and Carbon Ion Therapy*. Boca Raton: CRC Press; 2013.
128. Bolsi A, Lomax AJ, Pedroni E, Goitein G, Hug E. Experiences at the Paul Scherrer Institute with a remote patient positioning procedure for high-throughput proton radiation therapy. *Int J Radiat Oncol Biol Phys*. 2008;71:1581–1590.
129. Bissonnette JP, Balter PA, Dong L, et al. Quality assurance for image-guided radiation therapy utilizing CT-based technologies: a report of the AAPM TG-179. *Med Phys*. 2012;39:1946–1963.
130. Siochi RA, Balter P, Bloch CD, et al. Information technology resource management in radiation oncology. *J Appl Clin Med Phys*. 2009;10:16–35.
131. Digital Imaging and Communications in Medicine (DICOM). Supplement 11: Radiotherapy Objects; 1997.
132. Digital Imaging and Communications in Medicine (DICOM). *Supplement 102: Radiotherapy Extensions for Ion Therapy*; 2006.
133. Swerdloff SJ. Data handling in radiation therapy in the age of image-guided radiation therapy. *Semin Radiat Oncol*. 2007;17:287–292.
134. Bosch W, Curran B, Swerdloff S. IHE-RO: interoperable data standards for radiation oncology. In: Proceedings of the XVIth International Conference on the Use of Computers in Radiation Therapy (ICCR 2010), Amsterdam, The Netherlands. June 3, 2010; 2010.
135. Paganetti H, Niemierko A, Ancukiewicz M, et al. Relative biological effectiveness (RBE) values for proton beam therapy. *Int J Radiat Oncol Biol Phys*. 2002;53:407–421.
136. International Commission on Radiation Units & Measurements. Prescribing, Recording, and Reporting Proton-Beam Therapy (Report No. 78). Washington, DC: International Commission on Radiation Units and Measurements, Inc.;(2007). 78: Prescibing, Recording, and Reporting Proton-Beam Therapy.
137. Farr JB, Maughan RL. Dosimetry for proton and carbon ion therapy. In: Ma C-M, Lomax A, eds. *Proton and Carbon Ion Therapy*. Boca Raton: CRC Press; 2012:99–126.
138. Vynckier S. Dosimetry of clinical neutron and proton beams: an overview of recommendations. *Radiat Prot Dosimet*. 2004;110:565–572.
139. Andreo P, Burns D, Hohlfeld K, et al. TRS-398: Absorbed Dose Determination in External Beam Radiotherapy: An International Code of Practice for Dosimetry based on Standards of Absorbed Dose to Water (Technical Report Series 398). *International Atomic Energy Agency, Vienna*; 2001:420.
140. Brede HJ, Greif KD, Hecker O, et al. Absorbed dose to water determination with ionization chamber dosimetry and calorimetry in restricted neutron, photon, proton and heavy-ion radiation fields. *Phys Med Biol*. 2006;51:3667–3682.
141. Delacroix S, Bridier A, Mazal A, et al. Proton dosimetry comparison involving ionometry and calorimetry. *Int J Radiat Oncol Biol Phys*. 1997;37:711–718.
142. Medin J. Implementation of water calorimetry in a 180 MeV scanned pulsed proton beam including an experimental determination of k(Q) for a Farmer chamber. *Phys Med Biol*. 2010;55:3287–3298.
143. Palmans H, Seuntjens J, Verhaegen F, Denis JM, Vynckier S, Thierens H. Water calorimetry and ionization chamber dosimetry in an 85-MeV clinical proton beam. *Med Phys*. 1996;23:643–650.
144. Sarfehnia A, Clasie B, Chung E, et al. Direct absorbed dose to water determination based on water calorimetry in scanning proton beam delivery. *Med Phys*. 2010;37:3541–3550.

145. Jin H, Chen Y, Kendall E, Ahmad S. Commissioning of the compact pencil beam scanning proton beam therapy system. *JACMP*. 2019;19:94–105.
146. Muir BR, Cojocaru CD, McEwen MR, Ross CK. Electron beam water calorimetry measurements to obtain beam quality conversion factors. *Med Phys*. 2017;44:5433–5444.
147. Gomà C, Hofstetter-Boillat B, Safai S, Vörös S. Experimental validation of beam quality correction factors for proton beams. *Phys Med Biol*. 2015;60:3207–3216.
148. Medin J. Implementation of water calorimetry in a 180 MeV scanned pulsed proton beam including an experimental determination of kQ for a Farmer chamber. *Phys Med Biol*. 2010;55:3287–3298.
149. Lin L, Kang M, Solberg TD, et al. Use of a novel two-dimensional ionization chamber array for pencil beam scanning proton therapy beam quality assurance. *J Appl Clin Med Phys*. 2015;16:5323.
150. Seco J, Clasie B, Partridge M. Review on the characteristics of radiation detectors for dosimetry and imaging. *Phys Med Biol*. 2014;59: R303–R347.
151. Moyers MF, Vatnitsky SM. Radiation therapy with light ions. In: van Dyk J, ed. *The Modern Technology of Radiation Oncology: A Compendium for Medical Physicists and Radiation Oncologists*, 3rd edn. Madison, Wisconsin: Medical Physics Publishing; 2013:183–222.
152. Boag JW, Currant J. Current collection and ionic recombination in small cylindrical ionization chambers exposed to pulsed radiation. *Br J Radiol*. 1980;53:471–478.
153. Rossomme S, Delor A, Lorentini S, et al. Three-voltage linear method to determine ion recombination in proton and light-ion beams. *Phys Med Biol*. 2020;65:045015.
154. Liszka M, Stolarczyk L, Klodowska M, et al. Ion recombination and polarity correction factors for a plane-parallel ionization chamber in a proton scanning beam. *Med Phys*. 2018;45:391–401.
155. Mirandola A, Magro G, Maestri D, et al. Determination of ion recombination and polarity effect correction factors for a plane-parallel ionization Bragg peak chamber under proton and carbon ion pencil beams. *Phys Med Biol*. 2019;64:095010.
156. Vatnitsky S, Moyers M, Miller D, et al. Proton dosimetry inter-comparison based on the ICRU report 59 protocol. *Radiother Oncol*. 1999;51:273–279.
157. Farr JB, Mascia AE, Hsi WC, et al. Clinical characterization of a proton beam continuous uniform scanning system with dose layer stacking. *Med Phys*. 2008;35:4945–4954.
158. Nichiporov D, Kostjuchenko V, Puhl JM, et al. Investigation of applicability of alanine and radiochromic detectors to dosimetry of proton clinical beams. *Appl Radiat Isot*. 1995;46:1355–1362.
159. Summers P, Ibbott GS, Moyers MF, Grant RL, Followill DS. Comparison of clinical parameters for proton therapy in the United States. *Int J Radiat Oncol Biol Phys*. 2012;84:S30.
160. Newhauser WD, Durante M. Assessing the risk of second malignancies after modern radiotherapy. *Nat Rev Cancer*. 2011;11:438–448.
161. Ardenfors O, Dasu A, Lillhok J, Persson L, Gudowska I. Out-of-field doses from secondary radiation produced in proton therapy and the associated risk of radiation-induced cancer from a brain tumor treatment. *Phys Med*. 2018;53:129–136.
162. Brodin NP, Munck Af Rosenschold P, Aznar MC, et al. Radiobiological risk estimates of adverse events and secondary cancer for proton and photon radiation therapy of pediatric medulloblastoma. *Acta Oncol*. 2011;50:806–816.
163. Fontenot JD, Lee AK, Newhauser WD. Risk of secondary malignant neoplasms from proton therapy and intensity-modulated x-ray therapy for early-stage prostate cancer. *Int J Radiat Oncol Biol Phys*. 2009;74:616–622.
164. Fuji H, Schneider U, Ishida Y, et al. Assessment of organ dose reduction and secondary cancer risk associated with the use of proton beam therapy and intensity modulated radiation therapy in treatment of neuroblastomas. *Radiat Oncol*. 2013;8:255.
165. Paganetti H, Depauw N, Johnson A, Forman RB, Lau J, Jimenez R. The risk for developing a secondary cancer after breast radiation therapy: comparison of photon and proton techniques. *Radiother Oncol*. 2020;149:212–218.
166. Tamura M, Sakurai H, Mizumoto M, et al. Lifetime attributable risk of radiation-induced secondary cancer from proton beam therapy compared with that of intensity-modulated X-ray therapy in randomly sampled pediatric cancer patients. *J Radiat Res*. 2017;58:363–371.
167. Pérez-Andújar A, Newhauser WD, DeLuca PM. Contribution to neutron fluence and neutron absorbed dose from double scattering proton therapy system components. *Nucl Technol*. 2009;168:728–735.
168. Mukherjee B, Lambert J, Hentschel R, Farr J. Explicit estimation of out-of-field neutron and gamma dose equivalents during proton therapy using thermoluminescence-dosimeters. *Radiat Measur*. 2011;46:1952–1955.
169. Clasie B, Wroe A, Kooy H, et al. Assessment of out-of-field absorbed dose and equivalent dose in proton fields. *Med Phys*. 2010;37:311–321.
170. Kry S, Bednarz B, Howell RM, et al. *Report of the AAPM Task Group 158: Measurements and Calculations of Doses Outside the Treatment Volume from External Beam Radiation Therapy*. College Park, MD: American Association of Physicists in Medicine; 2017.
171. Moyers MF, Benton ER, Ghebremedhin A, Coutrakon G. Leakage and scatter radiation from a double scattering based proton beamline. *Med Phys*. 2008;35:128–144.
172. Zheng Y, Liu Y, Zeidan O, Schreuder AN, Keole S. Measurements of neutron dose equivalent for a proton therapy center using uniform scanning proton beams. *Med Phys*. 2012;39:3484–3492.
173. Wang X, Sahoo N, Zhu RX, Zullo JR, Gillin MT. Measurement of neutron dose equivalent and its dependence on beam configuration for a passive scattering proton delivery system. *Int J Radiat Oncol Biol Phys*. 2010;76:1563–1570.
174. Mesoloras G, Sandison G, Stewart R, Farr J, Hsi W-C. Neutron scattered dose equivalent to a fetus from proton radiotherapy of the mother. *Med Phys*. 2006;7:2479–2490.
175. Wang X, Poenisch F, Sahoo N, et al. Spot scanning proton therapy minimizes neutron dose in the setting of radiation therapy administered during pregnancy. *J Appl Clin Med Phys*. 2016;17:366–376.
176. Miften M, Mihailidis D, Kry SF, et al. Management of radiotherapy patients with implanted cardiac pacemakers and defibrillators: a report of the AAPM TG-203†. *Med Phys*. 2019;46:e757–e788.
177. Moyers MF, Toth T, Sadagopan R, et al. *Report of the AAPM Task Group 202: Physical Uncertainties in the Planning and Delivery of Light Ion Beam Treatments*. College Park, MD: American Association of Physicists in Medicine; 2017.
178. Zhu XR, Poenisch F, Lii M, et al. Commissioning dose computation models for spot scanning proton beams in water for a commercially available treatment planning system. *Med Phys*. 2013;40:041723.
179. Pedroni E, Scheib S, Böhringer T, et al. Experimental characterization and physical modelling of the dose distribution of scanned proton pencil beams. *Phys Med Biol*. 2005;50:541–561.
180. Schaffner B. Proton dose calculation based on in-air fluence measurements. *Phys Med Biol*. 2008;53:1545–1562.
181. Sawakuchi GO, Titt U, Mirkovic D, et al. Monte Carlo investigation of the low-dose envelope from scanned proton pencil beams. *Phys Med Biol*. 2010;55:711–721.
182. Hong L, Goitein M, Bucciolini M, et al. A pencil beam algorithm for proton dose calculations. *Phys Med Biol*. 1996;41:1305–1330.
183. Szymanowski H, Mazal A, Nauraye C, et al. Experimental determination and verification of the parameters used in a proton pencil beam algorithm. *Med Phys*. 2001;28:975–987.
184. Sawakuchi GO, Titt U, Mirkovic D, Mohan R. Density heterogeneities and the influence of multiple Coulomb and nuclear scatterings on the Bragg peak distal edge of proton therapy beams. *Phys Med Biol*. 2008;53:4605–4619.
185. Paganetti H, Jiang H, Parodi K, Slopsema R, Engelsman M. Clinical implementation of full Monte Carlo dose calculation in proton beam therapy. *Phys Med Biol*. 2008;53:4825–4853.
186. Yamashita T, Akagi T, Aso T, Kimura A, Sasaki T. Effect of inhomogeneity in a patient's body on the accuracy of the pencil beam algorithm in comparison to Monte Carlo. *Phys Med Biol*. 2012;57:7673–7688.
187. Schuemann J, Giantsoudi D, Grassberger C, Moteabbed M, Min CH, Paganetti H. Assessing the clinical impact of approximations in analytical dose calculations for proton therapy. *Int J Radiat Oncol Biol Phys*. 2015;92:1157–1164.
188. Han Y. Current status of proton therapy techniques for lung cancer. *Radiat Oncol J*. 2019;37:232–248.
189. Widesott L, Lorentini S, Fracchiolla F, Farace P, Schwarz M. Improvements in pencil beam scanning proton therapy dose calculation

accuracy in brain tumor cases with a commercial Monte Carlo algorithm. *Phys Med Biol*. 2018;63:145016.
190. Sorriaux J, Testa M, Paganetti H, et al. Experimental assessment of proton dose calculation accuracy in inhomogeneous media. *Phys Med*. 2017;38:10–15.
191. Lin L, Huang S, Kang M, et al. A benchmarking method to evaluate the accuracy of a commercial proton Monte Carlo pencil beam scanning treatment planning system. *J Appl Clin Med Phys*. 2017;18:44–49.
192. Inaniwa T, Kanematsu N, Hara Y, et al. Implementation of a triple Gaussian beam model with subdivision and redefinition against density heterogeneities in treatment planning for scanned carbon-ion radiotherapy. *Phys Med Biol*. 2014;59:5361–5386.
193. Clasie B, Depauw N, Fransen M, et al. Golden beam data for proton pencil-beam scanning. *Phys Med Biol*. 2012;57:1147–1158.
194. Kang M, Pang D. Commissioning and beam characterization of the first gantry-mounted accelerator pencil beam scanning proton system. *Med Phys*. 2019;47:3496–3510.
195. Anand A, Sahoo N, Zhu XR, et al. A procedure to determine the planar integral spot dose values of proton pencil beam spots. *Med Phys*. 2012;39:891–900.
196. Farr JB, Moskvin V, Lukose RC, Yao W, Schwamm F. Technical Note: design and characterization of a large diameter parallel plate ionization chamber for accurate integral depth dose measurements with proton beams. *Med Phys*. 2020;47:3214–3224.
197. Baumer C, Koska B, Lambert J, Timmermann B, Mertens T, Takoukam TP. Evaluation of detectors for acquisition of pristine depth-dose curves in pencil beam scanning. *J Appl Clin Med Phys*. 2015;16:151–163.
198. Fano U. Note on the Bragg-Gray cavity principle for measuring energy dissipation. *Radiat Res*. 1954;1:237–240.
199. Lin L, Ainsley CG, McDonough JE. Experimental characterization of two-dimensional pencil beam scanning proton spot profiles. *Phys Med Biol*. 2013;58:6193–6204.
200. Schwaab J, Brons S, Fieres J, Parodi K. Experimental characterization of lateral profiles of scanned proton and carbon ion pencil beams for improved beam models in ion therapy treatment planning. *Phys Med Biol*. 2011;56:7813–7827.
201. Braccini S, Ariga A, Ariga T, et al. Emulsion detectors for dose distribution characterization in the halo of proton pencil beams. *Strahlenther Onkol*. 2015;191:87.
202. Saini J, Cao N, Bowen S, et al. Clinical commissioning of a pencil beam scanning treatment planning system for proton therapy. *Int J Particle Ther*. 2016;3:51–60.
203. Nichiporov D, Hsi W, Farr J. Beam characteristics in two different proton uniform scanning systems: a side-by-side comparison. *Med Phys*. 2012;39:2559–2568.
204. Kramer M, Jäkel O, Haberer T, Kraft G, Schardt D, Weber U. Treatment planning for heavy-ion radiotherapy: physical beam model and dose optimization. *Phys Med Biol*. 2000;45:3299–3317.
205. Geng C, Moteabbed M, Xie Y, Schuemann J, Yock T, Paganetti H. Assessing the radiation-induced second cancer risk in proton therapy for pediatric brain tumors: the impact of employing a patient-specific aperture in pencil beam scanning. *Phys Med Biol*. 2016;61:12–22.
206. Wang D, Smith BR, Gelover E, Flynn RT, Hyer DE. A method to select aperture margin in collimated spot scanning proton therapy. *Phys Med Biol*. 2015;60:N109–N119.
207. Yasui K, Toshito T, Omachi C, et al. A patient-specific aperture system with an energy absorber for spot scanning proton beams: verification for clinical application. *Med Phys*. 2015;42:6999–7010.
208. Baumer C, Fuentes C, Janson M, Matic A, Timmermann B, Wulff J. Stereotactical fields applied in proton spot scanning mode with range shifter and collimating aperture. *Phys Med Biol*. 2019;64:155003.
209. Gillin MT, Sahoo N, Bues M, et al. Commissioning of the discrete spot scanning proton beam delivery system at the University of Texas M.D. Anderson Cancer Center, Proton Therapy Center, Houston. *Med Phys*. 2010;37:154–163.
210. Sawakuchi GO, Mirkovic D, Perles LA, et al. An MCNPX Monte Carlo model of a discrete spot scanning proton beam therapy nozzle. *Med Phys*. 2010;37:4960–4970.
211. Tanaka H, Takata T, Ishi Y, et al. Development of proton beam irradiation system for small animals using FFAG accelerator. *Nucl Instr Meth Phys Res A*. 2019;922:230–234.
212. Iqbal K, Gillin M, Buzdar SA, Summers PA, Dhanesar S, Gifford KA. Quality assurance evaluation of spot scanning beam proton therapy with an anthropomorphic prostate phantom using. *Br J Radiol*. 2013;86:20130390.
213. Albertini F, Casiraghi M, Lorentini S, Rombi B, Lomax AJ. Experimental verification of IMPT treatment plans in an anthropomorphic phantom in the presence of delivery uncertainties. *Phys Med Biol*. 2011;56:4415–4431.